TEKTONIKA

Testing the Sensitivity of Anisotropy of Magnetic Susceptibility (AMS) to the Regional Tectonic Strain Field in Granite Plutons; Insights from two Orogen-scale Studies

Hazel Knight *[1], **Carl Stevenson** [1], **Marco Maffione** [1], **William McCarthy** [2], **Alex Burton-Johnston** [3], **Anya Lawrence** [1]

[1]School of Geography Earth and Environmental Sciences, University of Birmingham, Birmingham, B15 2TT, UK | [2]Department of Earth & Environmental Sciences, University of St Andrews, St Andrews, Fife, KY16 9AL, UK | [3]British Antarctic Survey, High Cross, Madingley Road, Cambridge, CB3 0ET, UK

Abstract Anisotropy of Magnetic Susceptibility (AMS) fabrics within many individual granite plutons have previously been interpreted as recording the regional syn-magmatic tectonic strain field. To test this hypothesis, we compiled a regional database of AMS data from multiple granite complexes across two orogens, the French Massif Central and the British and Irish Caledonides. We critically evaluate the degree to which the magnetic fabric of the granite plutons recorded the known regional tectonic strain. AMS fabrics from nine plutons from the French Massif Central show that all intrusions recorded the syn-magmatic late Variscan extensional collapse, with the maximum susceptibility axes (i.e., magnetic lineation) aligned with the NW-SE regional stretching direction. AMS fabrics from ten late Caledonian 'Newer Granite' plutons appear to reliably record the changing tectonic regimes between 430 and 390 Ma, including the switch from transpression to transtension following Iapetus closure, and then the return to transpression following the onset of the Acadian Orogeny at 400 Ma. This study indicates that comparisons between AMS fabrics and regional tectonics is best achieved qualitatively by comparing the orientation of the susceptibility axes to the known strain field, and more quantitatively through Woodcock analysis. Overall, our results indicate that pluton-scale AMS fabrics from multiple complexes spaced across an orogen can record a complex and changing regional tectonic strain field. This indicates there is significant potential to utilise pluton-scale AMS studies, alongside precise geochronological ages, to refine the timings of an orogen's tectonic evolution.

Executive Editor:
Janine Kavanagh
Associate Editor:
Andy Parsons
Technical Editor:
Mohamed Gouiza

Reviewers:
Eric C. Ferré
Helena Silva
Rob Strachan

Submitted:
28 July 2023
Accepted:
30 July 2024
Published:
3 December 2024

1 Introduction

Mineral alignment fabrics are a common feature of granite plutons (e.g., *Marre*, 1986; *Bouchez*, 1997; *Pitcher*, 1997; *Paterson et al.*, 1998) and provide a record of syn- and post-magmatic strain. However, these fabrics are often too weak or subtle to be visible in the field. Anisotropy of Magnetic Susceptibility (AMS) is a petrofabric tool used to analyse such weak fabrics (e.g., *Tarling and Hrouda*, 1993; *Borradaile and Henry*, 1997). AMS represents an established structural analysis tool that allows the study of the syn-magmatic strain field, meaning if AMS fabrics can be reliably related to the regional tectonic strain field, granite plutons could represent extremely useful, directly ageable and short-lived kinematic markers in a region's tectonic evolution, providing better constraints on the timing and evolution of orogenic belts.

Over the last 30 years magnetic fabrics in several granite plutons have been interpreted as recording the regional tectonic strain active during their emplacement (*Archanjo et al.*, 1994; *de Saint Blanquat and Tikoff*, 1997; *Benn et al.*, 2001; *Talbot et al.*, 2005a; *Burton-Johnson et al.*, 2019) in a range of tectonic settings and geographic locations (*Burton-Johnson et al.*, 2019). *Benn et al.* (2001) proposed a regional scale extension of this type of analysis through 'mapping of magnetic fabrics in plutons of different ages within an orogenic belt to investigate the strain history during short periods' of the regional tectonic development. Whilst several regional scale studies have been completed, including *McCarthy* (2013) who demonstrated that combined AMS and U-Pb geochronology from multiple granitoid plutons within a complex spanning 423 to 380 Ma could be utilised to pin down transitions between regional stress fields during the late Caledonian orogeny, such studies are limited by the fact that they were

*✉ hkk761@student.bham.ac.uk

not expended to incorporate full regional dataset. Through the compilation of two regional-scale AMS databases, this project represents a step forward in testing the potential of granite intrusions to be used as a universal tool for studying the evolution of regional tectonic strain fields.

We have assembled a database of AMS data from granite bodies emplaced within the same spatial and temporal regions in two separate locations: the British and Irish Caledonides, and the French Massif Central. As the AMS tensor provides a reliable marker of relative strain magnitudes in three dimensions, we can compare the orientation and shape of this with the known syn-magmatic regional tectonic regime. This comparison allows us to assess the degree to which regional tectonic strain can be resolved by AMS and test the relative contribution of local strain heterogeneity (e.g., magmatic flow fabrics and shear zones).

2 Anisotropy of Magnetic Susceptibility: Background and Theory

2.1 Granite Fabrics

Fabrics defined by the syn-magmatic preferential alignment of mineral grains are common in granite plutons (e.g., *Bouchez*, 1997). Such fabrics form as a consequence of stresses exerted on the cooling magma, that cause grains to align with their long axis parallel to the maximum strain axis (*Paterson et al.*, 1998). Syn-magmatic stresses responsible for the development of magmatic state fabrics are numerous but can be broadly divided into: 1) internal magmatic body forces such as magmatic pressure or buoyancy and 2) the ambient regional tectonic strain field (*Paterson et al.*, 1998). Studies of individual granites have demonstrated that one of these can dominate the overall signal across a pluton, with either magma flow forming the dominant fabric (e.g., Trawengh Bay Granite; *Stevenson et al.*, 2007) or the overall fabric being dominated by regional tectonic stress (e.g., Margeride Granitic Complex; *Talbot et al.*, 2005a). However, many plutons have fabrics that do not dominantly record one of these sources, but instead reflects the interaction of regional tectonic stress and magma flow (e.g., The Ross of Mull Granite; *Petronis et al.*, 2012). Fabrics controlled by the regional tectonic stress are distinguished by the geometric continuity of the fabric inside the pluton with concurrent deformation fabrics in the surrounding host rocks; conversely, fabrics formed by magma emplacement show no relationship to host rock fabrics and a broader local variation within the pluton (*Paterson et al.*, 1998).

Granite magmas typically exist in the crust as a crystal-rich mush during a likely protracted emplacement period (*Cashman et al.*, 2017), with crystallisation occurring over a large range of temperatures, typically between 800 - 1000$^{\circ}C$ (with 2-5 wt% H_20) with the crustal-melt ratio still permitting flow as the body approaches the solidus (*Vigneresse et al.*, 1996; *Petford et al.*, 2000; *Vigneresse and Clemens*, 2000; *Petford*, 2003). The emplacement time scale may be protracted further by the melt remobilising during the intrusion of each pulse (*Cashman et al.*, 2017; *Sparks et al.*, 2019). During this protracted emplacement process, the intrusion may record multiple fabrics, which can be progressively replaced (e.g., *Paterson et al.*, 1998) or partially overprinted (*Petronis et al.*, 2012) upon changing stress conditions. When the melt finally approaches the solidus the most recent fabric is permanently "frozen" into the intrusion. Final magmatic fabrics therefore only record the final increments of strain (*Paterson et al.*, 1998) imparted as the crystal-mush approaches the solidus, with earlier strain overprinted by this final increment.

This means granite fabrics formed in response to regional tectonic stress represent extremely useful short-lived kinematic markers that record the palaeo-strain (*Paterson et al.*, 1998) at a specific of timepoint during an area's tectonic evolution. In this way granite fabrics have become strategic constraints for structural and tectonic analysis over the last 20 years (e.g., *Bouchez*, 1997; *Paterson et al.*, 1998; *Benn et al.*, 2001; *Burton-Johnson et al.*, 2019) helping to reconstruct the tectonic evolution of orogenic belts more accurately (e.g., *McCarthy*, 2013).

2.2 Anisotropy of Magnetic Susceptibility

Anisotropy of Magnetic Susceptibility can reveal the preferred orientation of minerals in a rock, through measuring the variations in magnetic susceptibility of an orientated sample in response to an externally applied magnetic field (*Jelínek*, 1977, 1978). The magnetic susceptibility (K) is the relationship between the strength of the applied filed (H) and the induced magnetism (M) formed in response, such that;

$$K = \frac{M}{H} \tag{1}$$

The susceptibility of a rock is controlled by its mineralogy, with different minerals exhibiting one of the three classes of magnetic behaviour: diamagnetism, paramagnatism or ferromagnetism.

Materials display a diamagnetic behaviour when the induced magnetism (M) shows a slightly negative non-permanent response to the applied field (H) (i.e., M decreases as H increases). Such behaviour arises as the spin of paired electrons flips to oppose the applied field. Diamagnatism dominates in most silicate minerals that do not contain iron in their crystal lattice, such as quartz, feldspars and calcite. Whilst these minerals are volumetrically significant in granite bodies, the weak nature of diamagnetic behaviour means the overall susceptibility of an igneous rock is instead dominated by paramagnetic

and ferromagnetic behaviour, even if such minerals are only present in very small quantities. It has been shown that 5 wt% paramagnetic grains or just 0.1-1 wt% ferromagnetic grains are enough to dominate the overall susceptibility (*Rochette*, 1987; *Tarling and Hrouda*, 1993; *Bouchez*, 1997).

Silicate minerals which do contain iron in their crystal lattice, such as biotite, clinopyroxenes or amphibole, instead show paramagnetic behaviour. In this case the induced susceptibility (M) has a positive, non-permanent response to the applied field (H). Such behaviour is strongly temperature dependant, with the susceptibility decreasing with increasing temperature according to the Curie law (see *Dunlop and Ozdemir*, 1997). Paramagnetic behaviour occurs due to a net magnetic moment caused by unpaired electrons reorientating in the same direction as the applied filed. These electrons are non-interacting, so the spins become randomised when the applied field is removed, meaning there is no remanent magnetism. The fact that the iron cations are distributed throughout the crystal lattice also means the magnetic anisotropy of paramagnetic minerals is itself controlled by the crystal lattice structure. So, only if the crystal axes are orthogonal will the measured principal susceptibility axes align with visible fabric formed by grain orientation. In sheet silicates such as biotite the α-axis is usually within 5° of principle susceptibility axis, meaning the measured susceptibility axis is a good proxy for grain alignment (*Borradaile and Henry*, 1997; *Borradaile and Jackson*, 2004). In contrast in minerals where the two axes do not align such as pyroxenes or amphiboles interpretation of the fabric is more complex (e.g., *Borradaile and Henry*, 1997).

The final category of magnetic behaviour is ferromagnetism where M shows a strongly positive proportional relationship to H, up to a maximum value, known as the saturation magnetism, and minerals may retain a remanent magnetism when subjected to a high field. Ferromagnetic behaviour in igneous rocks is almost always caused by magnetite, where closely coordinated Fe cations can interact across the crystal lattice, allowing the spins in neighbouring atoms to couple, giving an overall anisotropy which is controlled by the grain shape. Grain size also has an effect on magnetic behaviour, due to the presence of internal sub-grain magnetic domains, divided by Bloch walls. Within each domain electron spins are parallel, forming both an internal magnetic field and an equally sized external demagnetised field. A large external field is energetically inefficient, so to minimize this effect sub-grains are limited to around 0.1 μm. Grains larger than this will contain multiple domains and demonstrate 'Multi-domain' (MD) behaviour, where through the adjustment of Bloch walls the AMS fabric reflects the orientation of the mineral grain ('shape-preferred orientation' - SPO; *Bouchez*, 1997). Grains smaller than 0.1 μm only contain a single magnetic domain and therefore show 'Single-domain' (SD) behaviour where the AMS fabrics are instead perpendicular to the SPO (*Tarling and Hrouda*, 1993). Grains around 0.1 μm can show a combination of MD and SD behaviour, which is known as pseudo-single domain (PSD).

AMS measurements are represented as a magnetic susceptibility tensor: a second order symmetric matrix with three principal susceptibilities, $K_1 \geq K_2 \geq K_3$, corresponding to three mutually perpendicular principal axis directions (*Jelínek*, 1977). The AMS tensor is geometrically visualised as an ellipsoid with the three principal susceptibility axes, K_1, K_2, and K_3, corresponding to the long, intermediate, and short axis of the ellipsoid, respectively. The AMS ellipsoid can then be described through a set of three parameters, which respectively define its shape, size, and strength (or ellipticity) (*Jelínek*, 1978; *Tarling and Hrouda*, 1993).

Several AMS parameters have been suggested (*Tarling and Hrouda*, 1993), with the most commonly used outlined below. Ellipsoid size can be defined by the statistical mean susceptibility, K_{mean} (*Jelínek*, 1977; *Tarling and Hrouda*, 1993), as indicated in equation (2):

$$K_{mean} = \frac{K_1 + K_2 + K_3}{3} \tag{2}$$

Ellipsoid shape can be defined by the Shape Parameter (T) (*Jelínek*, 1978), as indicated in equation (3):

$$T = \frac{2(\ln K_2) - -\ln K_1 - \ln K_3}{\ln K_1 - \ln K_3} \tag{3}$$

T describes the shape of the ellipsoid as a numerical value between -1 and 1, where values of 1 and -1 represent a purely oblate and prolate ellipsoid, respectively, and T = 0 may then be regarded as triaxial (neither predominantly oblate or prolate). Ellipsoid strength is defined by the Corrected Degree of Anisotropy P_j (*Jelínek*, 1978), which is used over the Anisotropy Degree (P) as it also considers the intermediate axis K_2, as indicated in equations (4) and (5);

$$P_j = \sqrt{2((\ln K_1 - \eta m)^2 + (\ln K_2 - \eta m)^2 + (\ln K_3 - \eta m)^2)} \tag{4}$$

where

$$\eta m = \frac{\ln K_1 + \ln K_2 + \ln K_3}{3} \tag{5}$$

The magnetic Lineation (L) and magnetic Foliation (F) (*Tarling and Hrouda*, 1993) can be used alongside K_{mean} as an alternative trio of parameters to describe the ellipsoid (*Owens and Bamford*, 1976; *Owens*, 2000).

$$L = \frac{K_1 - K_2}{K_{mean}} \tag{6}$$

$$F = \frac{K_2 - K_3}{K_{mean}} \tag{7}$$

A plot of L vs F can be used for strain analysis where, in contrast to plotting P_j vs T, the small anisotropies

expected in plutonic fabrics can be viewed with similar error bars to large anisotropies. A final parameter H (*Tarling and Hrouda*, 1993) is often used in conjunction to describe the strength of the ellipsoid (see equation (8));

$$H = L + F = \frac{K_1 - K_3}{K_{mean}} \quad (8)$$

Overall, the magnitude of the principal susceptibility axes of the AMS tensor is usually a reliable indicator of relative strain magnitude in three-dimensions which, although is not a direct measurement of finite strain, is indicative of the strain. It must be noted that the magnetic fabric is also controlled by the type and shape of the rock-forming minerals, which may create a discrepancy between the AMS and strain ellipsoids. Within a coaxial strain field, the orientations of the principal susceptibility axis correspond to the direction of the principal strain axis during fabric formation, as shown in Figure 1 (*Burton-Johnson et al.*, 2019), where K_1 K_2 and K_3 are parallel with σ_3, σ_2 and σ_1 respectively.

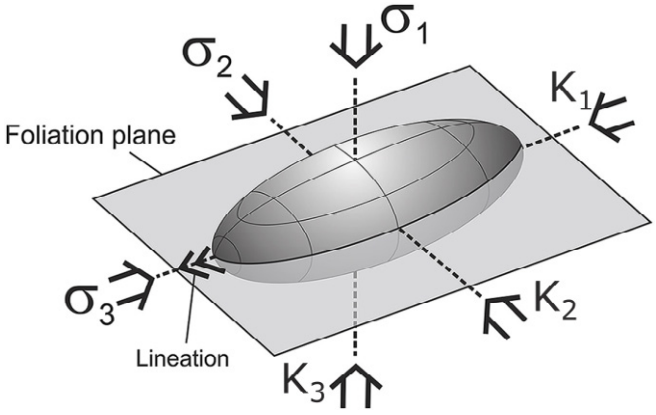

Figure 1 – Diagram from *Burton-Johnson et al.* (2019) illustrating the relationship between the three principal susceptibility axis to the syn-magmatic principal stress axis directions. K_1 = Maximum Susceptibility axis, K_2 = Intermediate Susceptibility axis and K_3 = Minimum Susceptibility axis. σ_1 = Maximum principal stress axis, σ_2 = Intermediate principal stress axis and σ_3 = Minimum principal stress axis. The susceptibility ellipse is shown along with the magnetic lineation (K_1) and foliation plane (plane perpendicular to K_3).

2.3 Stereographic Analysis of the AMS Axes

Due to the complex relationship between mineralogical magnetic behaviour, mineral preferred alignment and strain, AMS fabrics alone cannot be used to fully quantify the strain experienced by a pluton (*O'Driscoll et al.*, 2008). The orientations recorded by the AMS can be used to infer relative strain magnitude only when all other variables (including mineralogy, dominant magnetic carrier, pure vs simple shear, emplacement history) are first considered. This study compares the orientation and shape factors of the AMS fabrics systematically with the expected contemporaneous regional tectonic stress field, taking the fabric only as an indicator of relative strain magnitude in three-dimensions (as opposed to a direct measurement of strain).

AMS axes for each pluton were plotted on an equal area stereonet, such that all data for a pluton are shown on a single graph (i.e., one data point per site, representing the average value from all specimens analysed at that site (see Table 1), and Kamb contours were plotted. Contouring was calculated at three standard deviations for all plutons except the Glénat, Omps and Margeride two-mica granite plutons where, due to the low number of data points (<30), two standard deviation contours were more suitable. Contouring was plotted based on the assumption that the mineral fabric represents a single population and as such all data could be considered within the contouring. Whilst this assumption represents a clear simplification, with several of the original studies drawing out multiple fabric populations in the plutons, such as along shear zones (e.g., *McCarthy et al.*, 2015) or defined by discrete magma flow lobes (e.g., *Stevenson et al.*, 2007), this approach allowed us to provide a better assessment of the degree to which tectonically dominated fabrics prevail at a pluton scale. Contour distributions on these stereoplots were then used to analyse the shape of the fabric recorded by the AMS tensor. This was achieved by comparison to two end-members, with orientations plotting in one distinct region of the stereonet defined as a 'cluster' and orientations plotting along a great circle defined as a 'girdle' (as *Tarling and Hrouda*, 1993).

AMS axes distributions were then compared to the known contemporaneous regional strain field associated with a specific tectonic regime. Firstly, K_1 and K_3 orientations were compared to the direction of the regional tectonic lineation and foliation respectively. Secondly, the orientation (horizontal or vertical) of K_1 and K_3 were related to the corresponding principal strain axes (as Figure 2), then compared with the orientation of the principal strain axes expected from the regional tectonic regime. Thirdly, the distribution of data was considered, with clusters indicating a well-defined magnetic foliation or lineation. This record of the maximum strain axis can then be compared with the regional tectonic field.

As a first order conceptual model, two end-member scenarios can be considered where in extensional tectonic regimes a homogenous, ambient tectonic stretching would produce a cluster of K_1 orientations, whilst in compressive tectonic regimes a consistent maximum shortening direction would form a cluster of K_3 orientations. There of course exists other situations such as triaxial strain recorded with both K_1 and K_3 orientations forming clusters. Differences would also occur in heterogeneous settings, for example mid-crustal metamorphic terranes (e.g., the Himalaya *Parsons*

Table 1 – Summary information for the 18 plutons included in this study grouped by region. Sample sites represent discrete locations within a pluton where samples were collected, whilst the number of specimens per sample site represents the number of individual specimens taken at each of these locations by the original studies. Where clear data was not recorded in the original study the field has been left blank. [1]: pluton within Newary Igneous Complex. [2]: pluton within the Dongeal Batholith. [3]: The Margeride Granitic Complex. The latter is formed of two separate granites, an older facies known as the Porphyritic Granite (itself formed of the Margeride Granite and the Chambon le Chateau Granite) and a younger Saint-Christophe-d'Allier granite (*), which will be plotted separately.

Caledonian Newer Granites

Pluton	AMS Data Source	Location	Ages (Ma)	Age Data Source	Dating method (Isotope system (mineral, method))	Sample type (block vs field drilled)	Number of sample sites	Number of specimens (n) per sample site	Dominant magnetic carrier (as reported by original study)
Omey Pluton	*McCarthy et al.* (2015)	Northern Ireland	422.5 ± 1.7	*Feely et al.* (2007)	Re-Os (ID-TIMS)	Block sampled	113	Average 15	PSD to MD Titanomagnetite
Rathfriland Pluton[1]	*Anderson* (2015), *Anderson et al.* (2018)	Northern Ireland	414.02 ± 0.18 413.44 ± 0.37 412.53 ± 0.33 412.09 ± 0.36 411.94 ± 0.34 411.09 ± 0.18	*Anderson* (2015)	U-Pb (Zirocn, ID-TIMS)	Block sampled	35	8 -15	MD Magnetite
Newary Pluton[1]	*Anderson* (2015), *Anderson et al.* (2018)	Northern Ireland	410.29 ± 0.20 411.00 ± 0.58	*Anderson* (2015)	U-Pb (Zircon, ID-TIMS)	Block sampled	46	8 -15	MD Magnetite
Cloghoge Pluton[1]	*Anderson* (2015) *Anderson et al.* (2018)	Northern Ireland	407 ± 0.35	*Anderson* (2015)	U-Pb (Zircon, ID-TIMS)	Block sampled	22	8 -15	MD Magnetite
Ardara Pluton[2]	*Siegesmund and Becker* (2000)	Ireland	403.7 ± 8 431 to 424	*Siegesmund and Becker* (2000) *Archibald et al.* (2021)	K/Ar (Biotite) U-Pb (Zircon and titanite, LA-ICP-MS)	Block sampled	97	>3	Magnetite and Biotite
Rosses Granitic Complex[2]	*Stevenson* (2009)	Ireland	420 ± 6	*Archibald et al.* (2021)	U-Pb (Zircon, LA-ICP-MS)	Block sampled	57	6 - 12	Biotite
Trawenagh Bay Granite[2]	*Stevenson et al.* (2007)	Ireland	404 ± 10	*Archibald et al.* (2021)	U-Pb (Zircon, LA-ICP-MS)	Block sampled	152	6 - 12	Biotite and MD Magnetite
Ross of Mull Granite	*Petronis et al.* (2012)	Isle of Mull Scotland	425 ± 6	*McAteer* (2009)	U-Pb (Zircon, SIMS)	56 sites block sampled 83 sites field drilled	139	Field: 8 -14 Block: 8- 12	MD to PSD Titanomagnetite
Criffel Pluton	*Porter* (2002)	SW Scotland	418 ± 5 423 ± 4 416 ± 4 397 ± 2	*Oliver et al.* (2008) *Beckinsale and Obradovich* (1973) *Beckinsale and Obradovich* (1973) *Halliday et al.* (1980)	U-Pb (Zircon, LA-ICP-MS) K-Ar (Biotite) K-Ar (Amphibole) Rb-Sr (mineral-whole rock)	85 sites block sampled 71 field drilled	156	4 - 6	MD Magnetitie
Ratagain Complex	*Lawrence et al.* (2022)	NW Scotland	~365 408 – 416.8 415 ± 5 419 ± 3 425 ± 3	*Pidgeon and Aftalion* (1978) *Turnell* (1985) *Turnell* (1985) *Thirlwall* (1988) *Rogers and Dunning* (1991)	U-Pb (Biotite) Rb-Sr (Biotite-whole rock) Rb-Sr (Biotite-whole rock) Rb-Sr (Biotite-feldspar-whole rock) U-Pb (Baddeleyite, ID-TIMS)	Block sampled	100	3 - 10	MD Magnetite

et al., 2016) where tectonic transport in a shear zone records a stretching lineation even in a compression regime. However, following this first order view of the ambient strain field allows us a simplified starting point to compare pluton-scale AMS fabrics to the regional tectonics active at the time of emplacement. Finally, the degree of spread of data was analysed to assess the degree to which the AMS fabric effectively reflected the tectonic regime.

2.4 Ellipsoid Shape Analysis

Ellipsoid strength and shape parameters were analysed following the method of *Jelinek* (1981), using the P_j-T plot to visualise variability in ellipsoid strength and shape across multiple plutons. This analysis method was selected (as opposed to alternative parameters such as the magnetic lineation (L) and magnetic foliation (F); *Tarling and Hrouda*, 1993) as these parameters are most reported in the literature allowing a more complete regional database to be assembled. Where these parameters were not directly reported they were calculated if suitable data was available (K_1, K_2, K_3 and K_{mean} values), thus allowing P_j vs T plots to be generated for 15 of the 19 plutons in our dataset (required data was not available for the two plutons of the Margeride Granite Complex and the Criffel Pluton, and the Rosses Granitic Complex only has L and F parameters available). On such a plot the oblate and prolate fields are defined by T values between 0 and 1, and 0 and -1, respectively (*Jelinek*, 1981), while triaxial ellipsoids are characterised by samples with a T value close to zero (*Jelinek*, 1981). For each pluton with suitable data all data points were plotted on a single graph allowing the dominant ellipsoid shape at the pluton scale to be determined by assessing in which field (oblate vs prolate) data

Table 1 – Continued

Variscan Granites, French Massif Central

Pluton	AMS Data Source	Location	Ages (Ma)	Age Data Source	Dating method (Isotope system (mineral, method))	Sample type (block vs field drilled)	Number of sample sites	Number of specimens (n) per sample site	Dominant magnetic carrier (as reported by original study)
Millevaches Granite complex	*Gébelin et al.* (2006)	NW FMC	336 ± 7	*Monier* (1980)	Rb/Sr (Whole-rock)	Field drilled	105	5 -10	Biotite and Muscovite Mica
			332 ± 6	*Monier* (1980)	Rb/Sr (Whole-rock)				
			332 ± 15	*Augay* (1979)	Rb/Sr (Whole-rock)				
			357 ± 7	*Augay* (1979)	Rb/Sr (Whole-rock)				
Omps Pluton	*Joly et al.* (2009)	SW FMC	331.5 ± 3.5	*Joly et al.* (2009)	U-Th-Pb (Monazite, EPMA)	Field drilled	14	4 - 7	Biotite
Glénat Pluton	*Joly et al.* (2009)	SW FMC	320.8 ± 4.5	*Joly et al.* (2009)	U-Th-Pb (Monazite, EPMA)	Field drilled	14	4 - 7	Biotite
Margeride Granitic Complex[3]	*Talbot et al.* (2005a)	NW FMC	323 ± 12 314 ± 3	*Couturié et al.* (1979)	Rb/Sr (whole-rock)	?	210	4 - 12	Biotite
			334 ± 9	*Pin* (1979)	U/Pb (Monazite)				
			310 ± 3	*Respaut* (1984)	U/Pb (Zircon)				
			306 ± 3.1	*Monié et al.* (2000)	Ar/Ar (Biotite)				
			311 ± 6	*Isnard* (1996)	U/Pb (Monazite)				
			305 ± 14*	*Isnard* (1996)*	U/Pb* (Monazite)				Biotite and Muscovite*
Rocles Pluton	*Mezeme et al.* (2007)	Cévennes region, FMC	324 ± 4	*Mezeme et al.* (2007)	U-Th-Pb (Monazite, EPMA)	Field drilled	43	5 - 14	Biotite and Muscovite
			325 ± 4	*Mezeme et al.* (2007)	U-Th-Pb (Monazite, EPMA)				
			318 ± 5	*Mezeme et al.* (2005)	U-Th-PB (Monazite, EPMA)				
Mont Lorére-Borne Granitic complex	*Talbot et al.* (2004)	Cévennes region, FMC	315 ± 5	*Mialhe* (1980)	Rb-Sr (Whole-rock)	Field drilled	92	4 - 19	Biotite
			311 ± 3	*Monié et al.* (2000)	Ar/Ar (Biotite)				
			310 ± 3	*Monié et al.* (2000)	Ar/Ar (Biotite)				
			305 ± 5	*Monié et al.* (2000)	U-Pb (Monazite)				
			315 ± 4	*Monié et al.* (2000)	U-Pb (Monazite)				
Pont-de-Montvert-borne Pluton	*Talbot et al.* (2000)	Cévennes region, FMC	314 to 304	'Monié, per comms' in *Talbot et al.* (2000)	Ar/Ar (Biotite and Muscovite)	Field drilled	67	4 - 19	Biotite
			320 – 315	'Lancelot, per comms' in *Talbot et al.* (2000)	U-Pb (Zircon and Monazite)				
Aigoual-Saint Guiral-Liron Pluton	*Talbot et al.* (2005b)	Cévennes region, FMC	307 ± 3	*Monié et al.* (2000)	Ar/Ar (Biotite)	Field drilled	125	4 - 14	Biotite with hornblende and MD magnetite
			308 ± 3	*Monié et al.* (2000)	Ar/Ar (Biotite)				
			311 ± 3	*Monié et al.* (2000)	Ar/Ar (Biotite)				

points dominantly plot. It must be noted that the shape of the AMS ellipsoid can provide meaningful insight into the petrofabric only when the anisotropy degree is relatively high and is a function of the strain magnitude instead of the concentration of ferromagnetic minerals (i.e., when P and K_{mean} are not correlated). To assess this dependency data points were coloured by K_{mean} values where available.

2.5 Woodcock Analysis

The Woodcock analysis is a statistical method used to distinguish random distributions from statistically significant fabrics when analysing three-dimensional orientation data with a weak preferred orientation (*Woodcock and Naylor*, 1983). This allows the statistical quantification of the significance of a preferred orientation. This analysis was carried out following the methodology of *Woodcock and Naylor* (1983) for both K_1 and K_3 for each pluton.

Firstly, the mean orientation of the susceptibility tensor is defined in terms of three eigenvectors and three corresponding eigenvalues, representing the three principal axes of the data sample (Woodcock and Naylor, 1983). Eigenvalues were calculated by plotting the Bingham Axial Distribution, returning eigenvalues S1, S2 and S3, where the sum of S1 to S3 equals one (Woodcock and Naylor, 1983). Eigenvalues were calculated for K_1 and K_3 for each pluton studied.

Woodcock analyses were carried out for each pluton, with K_1 and K_3 values plotting as single data point for each pluton. The Woodcock plot then distinguishes random distributions from significantly orientated distributions, in the form of either a data girdle or cluster, to a certain confidence limit (*Woodcock and Naylor*, 1983). This is achieved through

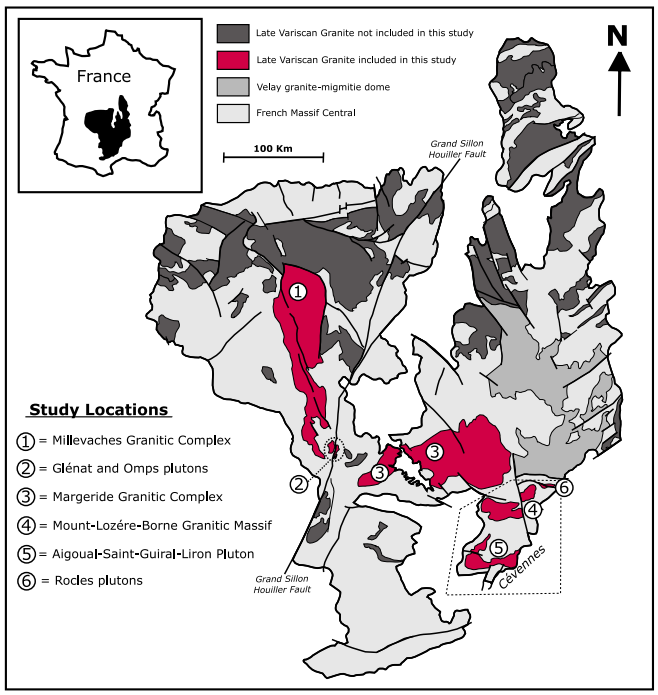

Figure 2 – Location map of the Late Variscan granite plutons within the French Massif Central. Plutons included in this study are shown in pink and numbered. Plutons of the same age but for which no suitable AMS data exists are shown in dark grey. The 300 Ma Velay migmatite dome is shown in light grey. The dotted line outlines the Cévennes region, for which the tectonic history differs. The Mont Lozère-Borne Granitic Complex contains the Pont-de-Montvert-Borne Pluton which is analysed separately (see *Faure et al.*, 2001), and the Margeride Granitic complex is split into the two-mica and porphyritic granites for analysis as the emplacement ages differ.

plotting a ratio graph, similar to a conventional Flinn plot, with the natural logarithm of S1/S2 on the y-axis and the natural logarithm of S2/S3 on the x-axis. The strength of a preferred orientation can also be determined on an eigenvalue ratio graph using the Strength Parameter, C (*Woodcock and Naylor*, 1983).

$$C = \ln \frac{S_1}{S_3} \tag{9}$$

The higher anisotropy a sample has, the larger the C value (i.e., further from the graph origin). This can therefore be used to assess the statistical significance of a preferred orientation. Woodcock and Naylor (1983) calculated critical values of C, for varying sample sizes (n), required to define a sample as statistically significant to various confidence limits using a Monte-Carlo framework. C values were calculated for each pluton and then compared to these critical values to assess whether AMS data recorded a statistically significant fabric at the pluton scale. Where statistically significant fabrics were identified at a pluton scale the shape of this fabric was further investigated on the eigenvalue ratio plot by calculating a Shape Factor, K (Woodcock and Naylor, 1983).

$$K = \frac{\ln \frac{S_1}{S_2}}{\ln \frac{S_2}{S_3}} \tag{10}$$

Where K = infinity represents a uniaxial cluster and K = 0 represents a uniaxial girdle. K values between 1 and infinity are considered the cluster field with K values less than 1 considered the girdle field. K is graphically the gradient of a line between the origin and a data point. For each study region the regional scale fabric shape was analysed by determining if K_1 and K_3 values dominantly plotted in the cluster or girdle field. The strength of this distribution (i.e., the K value) was also analysed. The distribution of a susceptibility axis as either a cluster or girdle was then related to strain, allowing woodcock plots for each region to be compared with the regional tectonic regime.

3 Regional Database Compilation and Geological Background

3.1 Region Selection

AMS datasets from multiple granites emplaced in the same spatial and temporal region were compiled into a comprehensive database. These fabrics were then compared based on the fundamental assumption that if AMS fabrics do reflect regional tectonic strain, then similar orientations would be recorded by AMS data to the expected tectonic trend. Furthermore, similarly oriented fabrics would be expected across individual granites emplaced in the same spatial and temporal region.

Study regions were selected based on (i) the availability of published AMS datasets for multiple granites within a spatial/temporal region and (ii) the understanding of the contemporaneous tectonic regime must be reasonably well documented to allow comparison with the AMS fabric. Two regions selected met these criteria: the late Variscan granites of the French Massif Central, which is a region with plentiful AMS datasets and a consistent and well-constrained contemporaneous tectonic regime, and the Caledonian 'Newer Granites' of Scotland and Ireland, which were emplaced during a well-documented change in tectonic regime associated with the final closure of the Iapetus Ocean. In particular, the study of the Newer Granites allowed us to assess the ability of AMS fabrics to record significant (and relatively rapid) changes in the regional tectonic regime.

To fully test whether the regional tectonic strain was recorded by AMS fabrics, data would ideally be compared from all plutons within the region. However, this was practically limited by the quantity and quality of the available data. Several criteria were required to be met before a dataset was suitable: firstly, fabrics must be demonstrably magmatic-state (i.e., formed during the primary emplacement/solidification) and not modified by

later deformation. Plutons containing a relatively small proportion of high temperature solid-state deformation, likely during the final stages of crystallisation and not significantly or pervasively overprinting the dominant magmatic state fabric have been included (e.g., Trawenagh Bay Granite (*Stevenson et al.*, 2007) and the Glénat Pluton (*Joly et al.*, 2009)). Secondly, orientation data pertaining to at least two principal susceptibility axes is required, ideally K_1 and K_3, though as all axes are mutually perpendicular any two are suitable as the third can be calculated. Information about the age of the pluton is also required to link it to contemporaneous tectonic events. Information about the mineral phase carrying the magnetic fabric is also required as this determines the relationship between the AMS fabric and the applied stress (e.g., *Tarling and Hrouda*, 1993; *Biedermann and Bilardello*, 2021). All plutons included in our database have AMS fabrics originally interpreted as parallel to the mineral alignment and therefore the strain field, allowing direct comparison within this study. Table 1 shows that for the majority of our plutons the reported dominant carrier of the AMS fabric is either multi-domain (MD) magnetite or biotite, both of which result in magnetic susceptibility controlled by grain shape and therefore grain orientation (see Section 2.2). Whilst considering the fabric based on the dominant carrier is a clear simplification of the overall fabric, which will be the result of many different mineral contributions (e.g., *Talbot et al.*, 2005a; *Anderson et al.*, 2018) that may even vary across different facies within the individual granites (e.g., *Siegesmund and Becker*, 2000), it allows a simple verification of this assertion and clearer comparison across many different granite bodies. Therefore, based on this assertion from the original studies, we can use the AMS fabric as a proxy for the mineral alignment. Whilst we do not suggest that the mineralogical assemblage is a uniform indicator of magmatic strain, we instead simply use the orientation data to provide a generalised view of the stain field.

Following this assessment, a dataset from 19 suitable plutons was compiled (Table 1). AMS data were reported for between 22 and 210 sites within these plutons, with the values reported for each site being calculated from between 4 and 19 individual specimens. As more studies reported site-mean average values than individual specimen values, only the site averages were compiled into our dataset, to allow direct comparison between all the plutons. Therefore, in our database a single data point for a pluton represents an average value of up to 19 individual specimens.

3.2 French Massif Central

The Variscan Orogeny occurred during the late Palaeozoic due to the collision of Gondwana and Laurussia (e.g., *Schulmann et al.*, 2022). The French Massif Central (FMC), formed as part of the Variscan belt of western Europe, is composed of a stack of metamorphic nappes (*Faure et al.*, 2005) formed on the northern margin of Gondwana between the Late Devonian and Middle Carboniferous (*Talbot et al.*, 2005b). Common with many orogenic belts, crustal thickening resulted in partial melting of the crust and gravitational instability (*Faure*, 1995). Because of this gravitational instability the Middle to Late Carboniferous in the FMC is dominated by late orogenic extensional collapse and voluminous granitic intrusions (*Faure*, 1995; *Faure et al.*, 2005; *Talbot et al.*, 2005b; *Gébelin et al.*, 2006). Extension occurred in two successive phases (*Faure*, 1995) with the first phase being characterised by orogen parallel NW-SE directed extension (*Talbot et al.*, 2005a; *Gébelin et al.*, 2006; *Joly et al.*, 2009). The onset of this extension was diachronous across the region, beginning earlier in the North in the late Visean around 330 Ma. Extension then shifted southwards, with the entire region undergoing extension by around 320 Ma (*Talbot et al.*, 2000) though the precise timing of the southward propagation is not well constrained (*Talbot et al.*, 2005a).

Extension continued across the entire FMC until 310 to 300 Ma (*Talbot et al.*, 2000; *Faure et al.*, 2005), with a consistent NW-SE directed maximum stretching direction across the main FMC region (*Joly et al.*, 2009). In contrast, the Cévennees area (Figure 2) in the far SE of the FMC underwent E-W to NW-SE directed extension from 320 to 305 Ma (*Talbot et al.*, 2000; *Faure et al.*, 2001; *Talbot et al.*, 2005b). Across the FMC, this extension was coeval with granite magma emplacement, with the majority of plutons emplaced between 325 and 310 Ma (*Faure et al.*, 2005). A second phase of extension occurred in the late Carboniferous to early Permian (*Talbot et al.*, 2005a; *Gébelin et al.*, 2006) across the entire FMC, characterised by a N-S to NE- SW directed stretching. The Velay migmatite dome was emplaced in this tectonic regime at 300 Ma before late-orogenic extension ended at 290 Ma (*Joly et al.*, 2009).

3.3 Caledonian 'Newer Granites' of Scotland and Ireland

The Caledonian orogeny encompassed what is currently NW Scotland, Ireland and Scandinavia occurring as the result of the collision between Laurentia in the West, Avalonia in the East and Baltica in the North. Northward directed subduction of the Iapetus Ocean continued until final closure in the late Silurian to early Devonian (*Woodcock and Strachan*, 2012) resulting in the formation of the Caledonian mountain belt and the Southern Uplands accretionary prism, as well as volumetric granitic magmatism. The oblique nature of convergence (*Soper and Woodcock*, 2003) implied that final continental collision occurred by sinistral 'soft-docking' between 425 and 420 Ma (*Soper and Woodcock*, 2003; *Dewey and Strachan*, 2003; *Brown et al.*, 2008). In Scotland and Ireland, the period following final convergence is characterised by alternating tectonic regimes (*Woodcock and Strachan*,

2012), coeval with widespread granite emplacement. Regional transpression ended with final continental collision and was followed by a period of orogen-wide sinistral transtension that occurred from 419 Ma (*Miles et al.*, 2016; *Miles and Woodcock*, 2018) to 400 Ma. This was terminated by the onset of the Acadian orogeny at around 400 Ma, which led to the development of regional transpression for around 10 Ma (*Soper and Woodcock*, 2003; *Brown et al.*, 2008).

The Caledonian 'Newer Granites' represent a suite of calc-alkaline granite plutons formed between 435 and 380 Ma (e.g., *Atherton*, 2002; *Brown et al.*, 2008; *Searle*, 2022), spanning this period of tectonic changes, with magmatism occurring on both siydes of the newly formed Iapetus suture (*Soper and Woodcock*, 2003). An increase in magma generation occurred following the onset of Devonian transtension, when slab break off resulted in uplift (*Atherton*, 2002; *Neilson et al.*, 2009; *Miles et al.*, 2016) and crustal thinning, which triggered lamprophyre melting and upper-crustal granitic melt generation (*Brown et al.*, 2008). Emplacement was then facilitated tectonically, through shear zones (e.g., *Jacques and Reavy*, 1994) that developed in response to regional sinistral transpression (*Brown et al.*, 2008).

4 Results

4.1 Variscan French Massif Central

A total of nine suitable plutons with appropriate AMS data were found for the French Massif, spanning the period of late Variscan orogenic collapse between 330 and 290 Ma. The location of the studied plutons is shown in Figure 2. Of these nine plutons, five were emplaced between 335 and 305 Ma in the main part of the FMC, whilst the remaining four are located in the far SE Cévennes region. These formed later, between 320 and 300 Ma, as extension shifted southward. Results for the main FMC granites are shown in Figure 3 and for Cévennes region granites in Figure 4. Full data sets are available in Appendix A. For the Omps and Glénat plutons only K_1 and K_2 orientations were reported so K_3 orientations plotted below are calculated values using the mutually perpendicular relationship between the three axes (calculations in Appendix A). P_j-T plots are shown for all plutons except the Margeride Granitic Complex, where data is not available.

The Millevaches Granitic Complex: Stereonets in Figure 3a show pluton scale AMS data for the Millevaches Granitic Complex records horizontal K_1 (Figure 3ai) and sub-vertical K_3 orientations (Figure 3aii). Data spread is noticeable but overall K_1 orientations define a cluster near the perimeter, directed NW-SE, whilst K_3 orientations define an approximate girdle, directed NE-SW. Shape factor analysis (Figure 3aiii) show a predominance of oblate ellipsoids recorded by individual samples, with the majority of samples plotting in the oblate field, and the samples with the strongest degree of anisotropy (highest P_j values) also in the oblate field.

The Omps Pluton: Stereonets of K_1 and K_3 for the Omps Pluton are shown in Figure 3b. The low number of data points available increases uncertainty, with contouring calculated to a lower degree of significance to account for this. K_1 orientations are spread, neither defining a clear girdle or cluster, with contorting indicating a NW-SE sub-horizontal direction (Figure 3bi), though five sites show a steep mean K_1. Inferred K_3 orientations are shallowly plunging and NE-SW distributed (Figure 3bii). Shape factor analysis (Figure 3biii) shows the majority of samples plot within the oblate field. However, the two samples with the highest anisotropy degree plot in the prolate field.

The Glénat Pluton: Stereonets of K_1 and K_3 distributions for the Glénat Pluton are shown in Figure 3c. K_1 orientations are sub-horizontal, with a significant spread of data (Figure 3ci). Inferred K_3 orientations are well-clustered and shallowly plunging towards the NE (Figure 3cii). Shape factor analysis (Figure 3ciii) shows all samples except one plot within the oblate field.

The Margeride Granitic Complex: The Margeride Granitic complex is composed of three plutons, formed in two stages with a 10 Ma interval (*Talbot et al.*, 2005a). Results for the younger porphyritic monzogranite facies, formed of the Margeride Granite and the Chambon le Chateau Granite, are shown in Figure 3d. Overall, there is significant data spread but contouring indicates that K_1 orientations define a sub-horizontal NW-SE cluster of data (Figure 3ai). K_3 orientations are largely scattered but form a predominantly vertical distribution, potentially in the form of a NE-SE directed girdle (Figure 3dii). No ellipsoid shape data is available for this complex.

The Saint-Chritsophe-d'Allier Two-mica Granite: Results for the younger Saint-Christophe-d'Allier Two-mica Granite are shown in Figure 3e. The number of data points available for this pluton is limited so contouring was plotted to a lower significance. K_1 orientations are extremely similar to the porphyritic facies, forming a NW-SE directed, sub-horizontal cluster (Figure 3ei). K_3 orientations form a poorly-defined a girdle, as seen in the older porphyritic facies, but with a N-S trend, though this may be an effect of the low number of samples (Figure 3eii). No ellipsoid shape or strength data is available for this complex

The Rocles Pluton: Results for the Rocles Pluton, the oldest pluton studied within the Cévennes region, are shown in Figure 4a. K_1 orientations are NE-SW directed, form a cluster and are horizontal to sub-horizontal (Figure 4ai). K_3 orientations also form a sub-horizontal cluster (Figure 4aii). However, the Rocles pluton was tilted to the South by the later emplacement of the adjacent Velay Migmatite

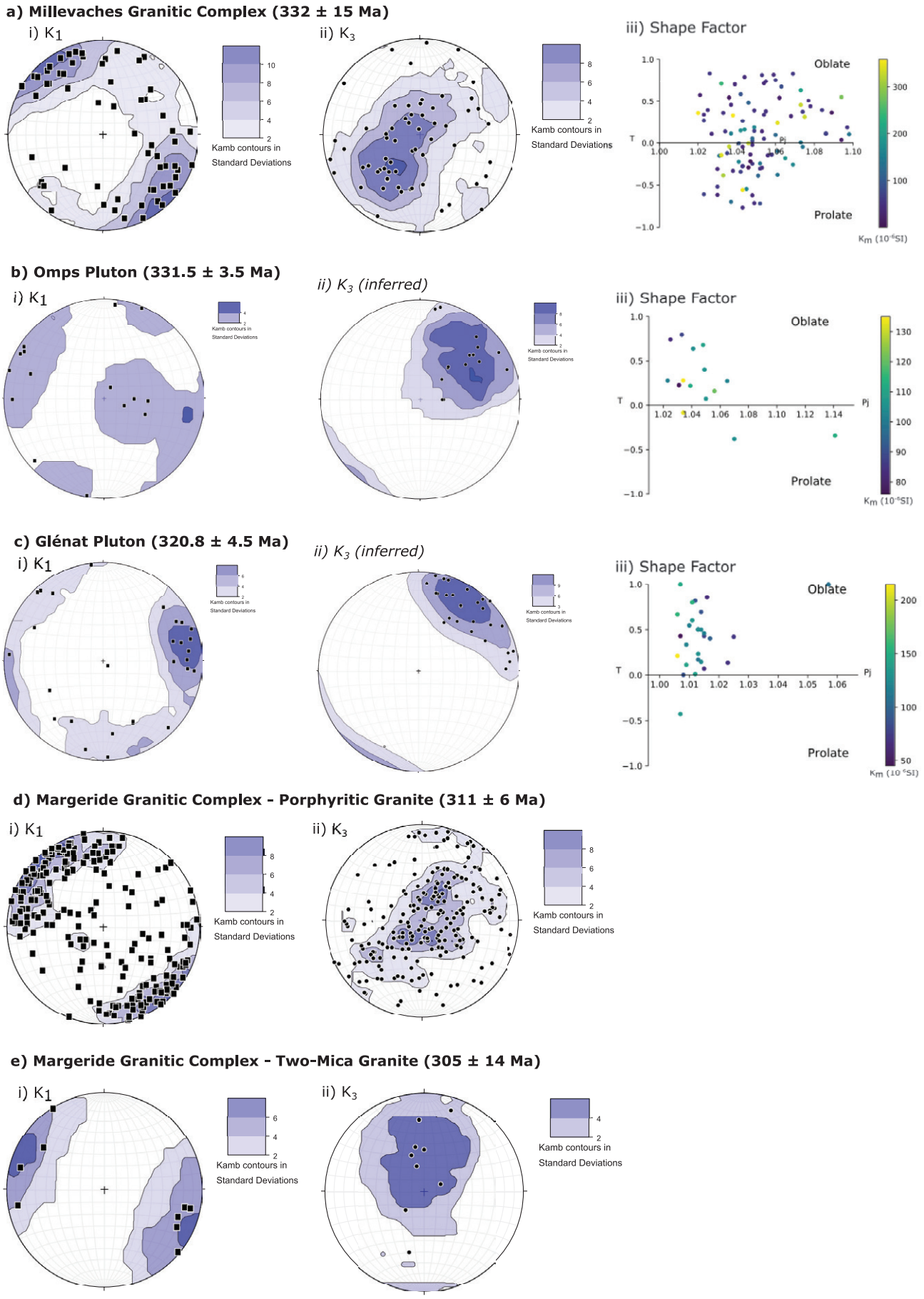

Figure 3 – Lower hemisphere equal area projections of K_1 and K_3 susceptibility axes and ellipsoid parameter plots for the five central French Massif Central (FMC) granites used in this study where i) =Lineation (K_1 values), ii) =Pole to foliation (K_3 values) and iii) = P_j vs T graph. Data sources are as follows: Millevaches Granitic Complex: *Gébelin et al.* (2006); Omps Pluton: *Joly et al.* (2009) Joly et al (2009); Glénat Pluton: *Joly et al.* (2009); Margeride Granitic Complex: *Talbot et al.* (2005a).

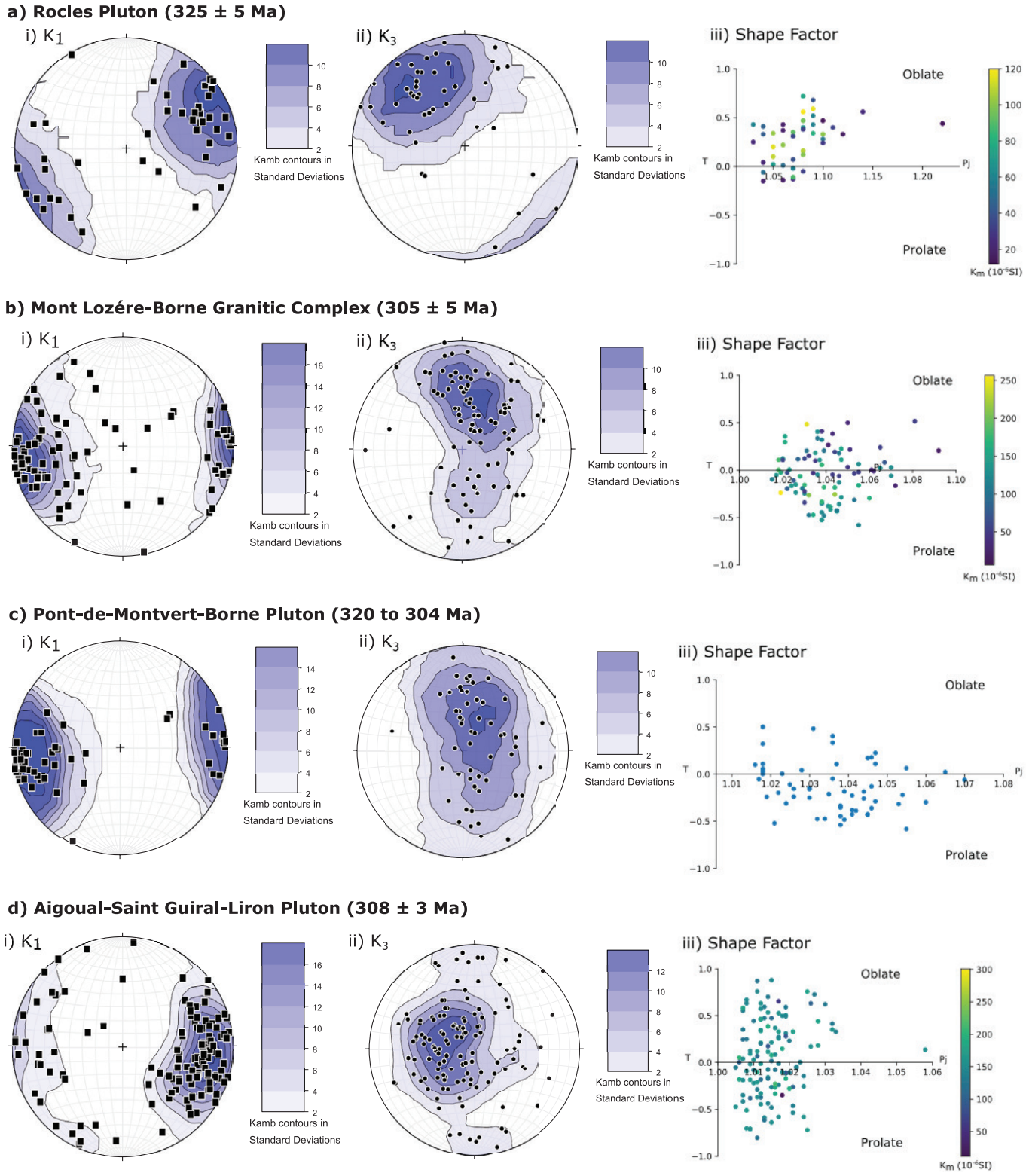

Figure 4 – Lower hemisphere equal area projections of K_1 and K_3 susceptibility axis orientation and ellipsoid parameter plots for the four granites used in this study from the Cévennes region of the French Massif Central (FMC)where i) =Lineation (K_1 values), ii) =Pole to foliation (K_3 values) and iii) = P_j vs T graph. The Roccles pluton (4a) is was tilted during the emplacement of the Velay migmatite dome meaning the orientation recorded here does not represent the orientation of the fabric at the time of emplacement. Data sources are as follows: Rocles Pluton: (*Mezeme et al.*, 2005); Mont-Lozére-Borne Granitic Complex: *Talbot et al.* (2004); Pont-de-Montvert-Borne Pluton: *Talbot et al.* (2000); Aigoual-Saint Guiral-Liron Pluton: *Talbot et al.* (2005b).

Dome (*Mezeme et al.*, 2007) (Figure 2). This means the measured fabric orientation is not the same as the orientation of the primary fabric at the time of formation, so these results require further interpretation. Shape factor analysis (Figure 4aiii) shows a clear dominance of oblate ellipsoids.

The Mont Lozére-Borne Granitic Complex: The Mont Lozére-Borne Granitic Complex is composed of the Mont Lozére Massif and the Borne Massif (*Faure et al.*, 2001). Results are shown in Figure 4b. K_1 orientations are dominantly horizontal, with data forming a very distinct E-W directed cluster (Figure 4bi). K_3 orientations define a clear N-S girdle and are dominantly sub-horizontal (Figure 4bii). Shape factor analysis (Figure 4bii) shows individual samples record oblate and prolate ellipsoid fairly evenly, with data mainly clustering around the x-axis (T = 0), suggesting triaxial ellipsoids dominate (Figure 4biii).

The Pont-de-Montvert-Borne Pluton: The Pont-de-Montvert-Borne Pluton is formed of the Pont-de-Montvert granite and the Borne Granite, which also forms a component of the Borne Massif (*Faure et al.*, 2001). Results are shown in Figure 4c. K_1 orientations are predominantly horizontal and define a distinct E-W cluster (Figure 4cii), though slightly more ENE-WSW than the related Mont Lozére-Borne complex. K_3 orientations define a clear N-S girdle distribution (Figure 4cii). Shape factor analysis (Figure 4ciii) shows a slight dominance of prolate ellipsoids, though the majority of the data points plot near the x-axis, indicating a triaxial component. However, these samples have a very low degree of anisotropy (P_j < 1.1), meaning very slight variations can shift the values, so such conclusions are less meaningful. The highest anisotropy samples are seen in both the oblate and prolate field, again suggesting variability in individual samples here.

The Aigoual-Saint Guiral-Liron Pluton: Results for the Aigoual-Saint Guiral-Liron Pluton are shown in Figure 4d. K_1 orientations are dominantly horizontal, orientated E-W, and define a data cluster (Figure 4di), though this is more spread than for the other Cévennes region granites. K_3 orientations form a poorly defined N-S directed gridle, with a predominance of vertical orientations (Figure 4dii). Shape factor analysis (Figure 4diii) shows a fairly even distribution of sample results between oblate and prolate fields, though the highest degrees of anisotropy are seen within samples in the oblate field.

Overall results from the FMC indicate horizontal K_1 and vertical K_3 orientations dominate across the plutons. Results also show two main populations with plutons in the main FMC area mostly characterised by NW-SE directed lineation's (K_1) and NE-SW directed pole to foliations (K_3). In contrast plutons within the Cévennes region are characterised by E-W directed lineation's (K_1) and N-S directed pole to foliations (K_3). Notable exceptions to this are the Rocles pluton (Figure 4a), which can be explained in terms of subsequent tilting, and the Glénat Pluton (Figure 3c), which does not record a clear NW-SE lineation, but a spread of low angle K_1 values. P_j vs T plots show dominantly oblate ellipsoids recorded by individual samples, with a more triaxial component in the Cévennes region.

4.2 Caledonian Newer Granites of Scotland and Ireland

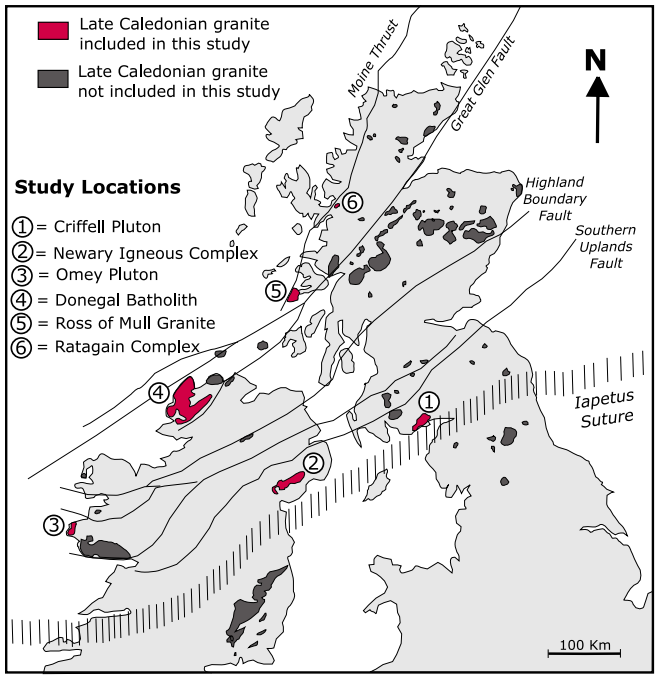

Figure 5 – Location map of the Caledonian Newer Granites suite granite plutons across Scotland, Ireland, and Northern Ireland. Plutons included in this study are shown in pink and numbered. Plutons of similar age but for which no suitable AMS data exists are shown in dark grey. Key terrain bounding faults and the Iapetus suture are labelled. The Donegal batholith is split into the Trawenagh Bay Granite, the Rosses Granitic Complex and the Adara Pluton for analysis. The Newary Igneous complex is split into the Cloghoge pluton, the Newary Pluton and the Rathfriland pluton for analysis.

Ten plutons with appropriate AMS data were selected from the Caledonian Newer Granites intrusive suite of Scotland and Ireland. These span the late Caledonian tectonic changes between 430 and 390 Ma, following final closure of the Iapetus Ocean (e.g., *Woodcock and Strachan*, 2012). The location of the studied plutons is shown on Figure 5. Stereonets of K_1 and K_3 orientations have been plotted for all plutons, shown in Figure 6. P_j-T plots are also shown in these figures, with the exception of the Rosses Granitic Complex, where only data for the comparable L-F plot was available, and the Criffel Pluton, where no ellipsoid shape data were available. Full datasets are included in Appendix B, with results for each pluton explained below.

The Omey Pluton: AMS data for the Omey Pluton show NW-SE oriented girdle of K_1 orientations (Figure 6ai), with predominantly moderate plunging directions. K_3 orientations are sub-horizontal,

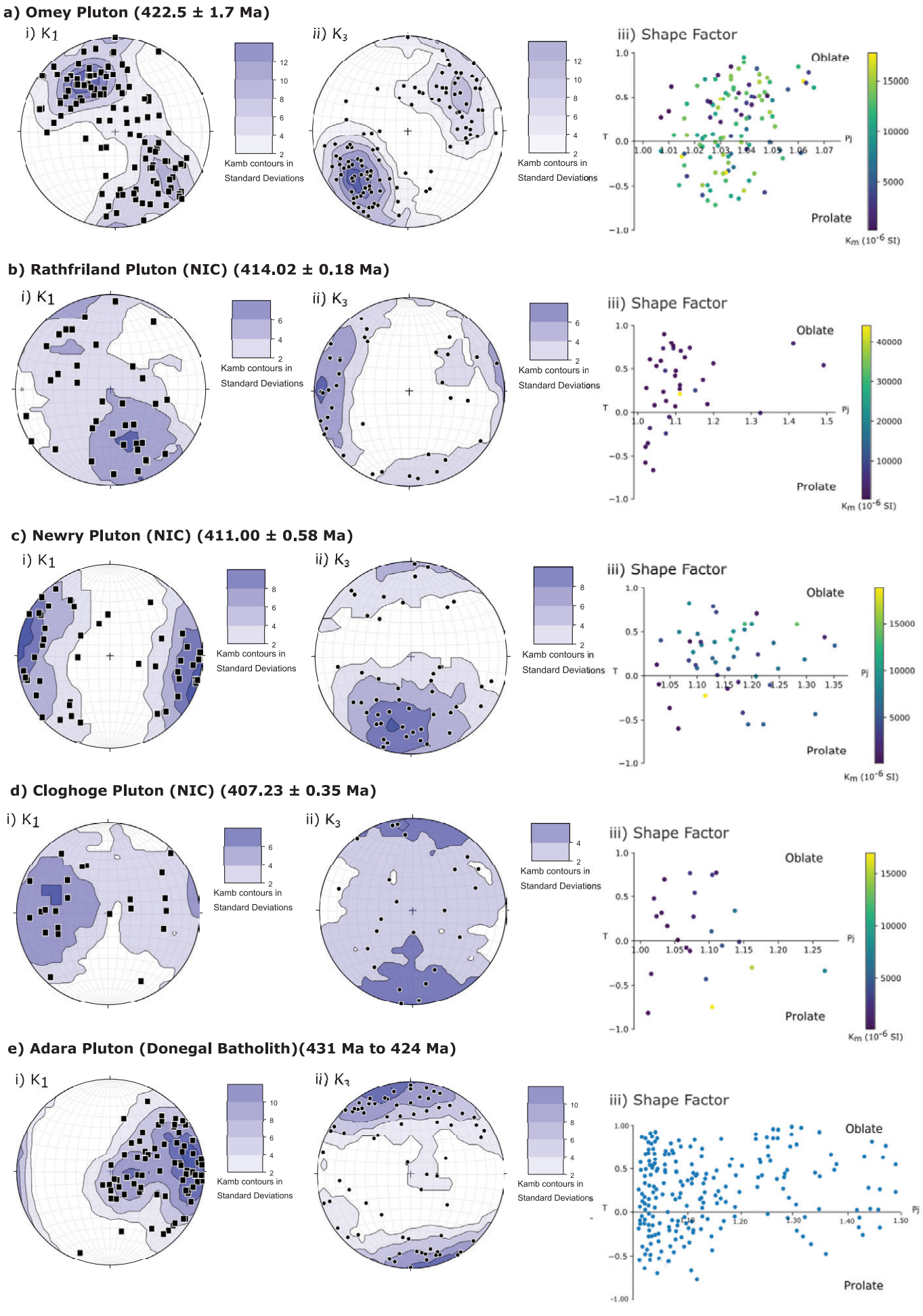

Figure 6 – Continued

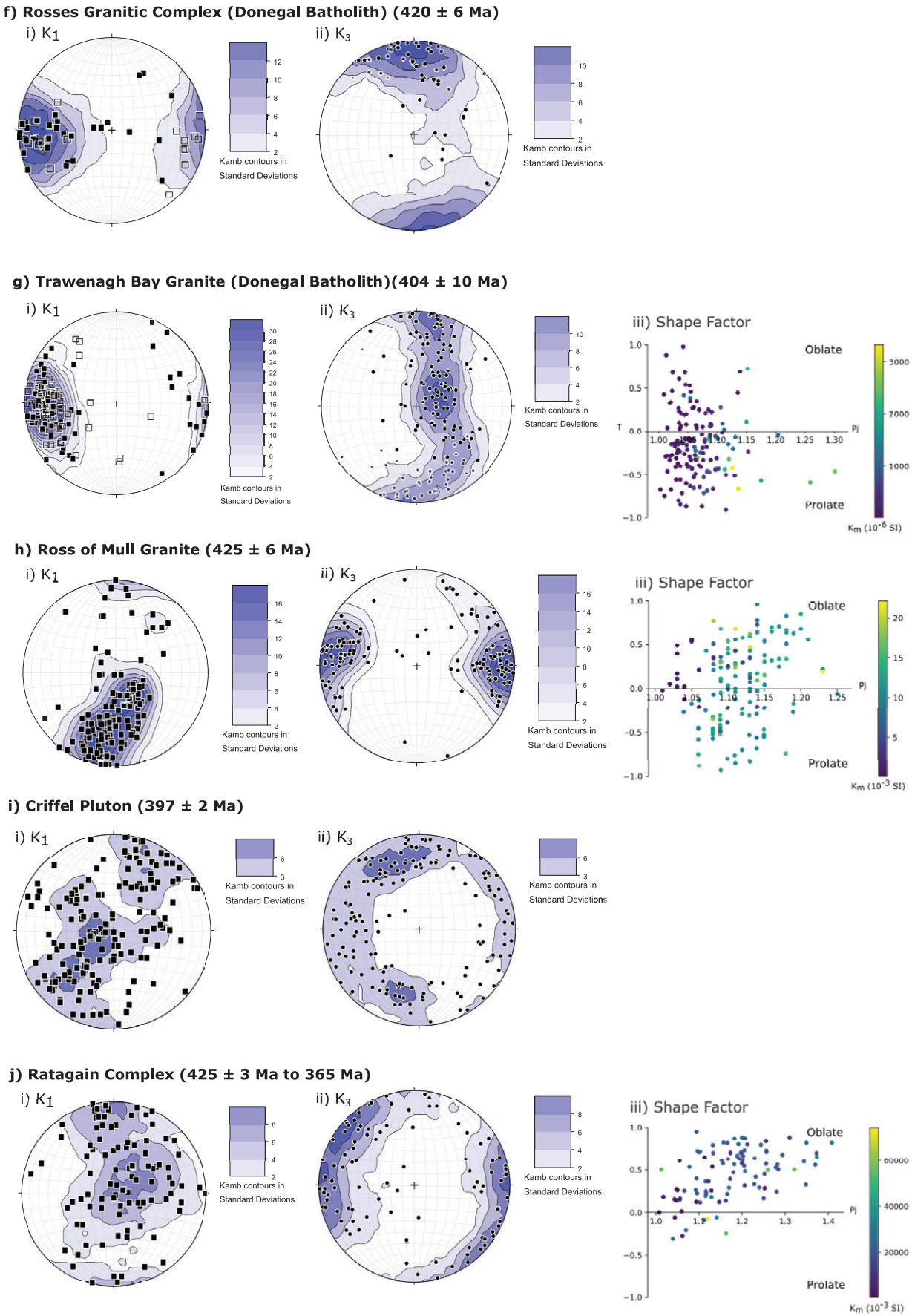

Figure 6 – Lower hemisphere equal area projections of K_1 and K_3 susceptibility axis orientation and ellipsoid parameter plots for the ten granites used in this study from the Caledonian Newer Granites suite across Scotland, Ireland and Northern Ireland where i) =Lineation (K_1 values), ii) =Pole to foliation (K_3 values) and iii) P_j vs T graph. Data sources are as follows: Omey Pluton: *McCarthy et al.* (2015); Rathfriland Pluton, Newry Pluton, Cloghoge Pluton: *Anderson et al.* (2018); Adara Pluton: *Siegesmund and Becker* (2000); Rosses Granitic Complex: *Stevenson* (2009); Trawenagh Bay Granite: *Stevenson et al.* (2007); Ross of Mull Granite: *Petronis et al.* (2012); Criffel Pluton: *Porter* (2002); Ratagain Complex: *Lawrence et al.* (2022).

forming data clusters orientated NE-SW (Figure 6aii). Shape factor analysis (Figure 6aiii) shows a slight dominance of oblate ellipsoids, with the most anisotropic values also plotting in the oblate field. However, there is also a notable number of individual sites recording prolate ellipsoids.

The Rathfriland Pluton (Newry Igneous Complex): Data for the Rathfriland pluton, the oldest component of the Newry Igneous Complex, is shown in Figure 6b. K_1 orientations define a poorly-developed NNW-SSE girdle (Figure 6bi), though there is significantly more spread in data compared with other plutons. K_3 orientations show a relatively large scatter in azimuth but a consistent sub-horizontal plunge (Figure 6aii). With contouring showing a slight E-W clustering. Shape factor analysis (Figure 6biii) shows a significant dominance of samples plotting within the oblate field, including two strongly anisotropic samples. Only a few low anisotropy samples plot in the prolate field.

The Newry Pluton (Newry Igneous Complex): Stereonets shown in Figure 6c, indicate distinct differences between the Newry pluton and the younger Rathfriland pluton. At a pluton scale AMS data shows K_1 orientations forming an approximately E-W orientated, horizontal cluster (Figure 6ci). K_3 orientations (Figure 6cii) cluster towards the South with an average sub-horizontal plunge. Shape factor analysis shows a dominance of samples in the oblate field (Figure 6ciii).

The Cloghoge Pluton (Newry Igneous Complex): The youngest component of the Newry Igneous Complex is the Cloghoge pluton, results for which are shown in Figure 6d. K_1 orientations are relatively scattered but form a slight shallowly plunging cluster towards the West (Figure 6di). The same is seen for K_3 orientations, where contouring indicates a poorly-defined N-S trending, horizontal cluster (Figure 6dii). Shape factor analysis also shows a range of ellipsoid shapes recorded by individual samples, with samples dominantly plotting in the oblate field, though the two samples with the greatest anisotropy degrees plot in the prolate field (Figure 6diii).

The Ardara Pluton (Donegal Batholith): Results for the Ardara Pluton, the youngest component of the 400 Ma Donegal Batholith, are shown in Figure 6e. K_1 orientations define a good data cluster, horizontal and ENE-WSW trending (Figure 6ei). K_3 orientations are more dispersed but are horizontal and N-S directed, mostly plot close to the perimeter (Figure 6eii). Shape factor analysis for individual sites shows that oblate ellipsoids are predominantly recorded, with a large number of sites recording high degrees of anisotropy (Figure 6eiii), compared with other plutons studied.

The Rosses Granitic Complex (Donegal Batholith): The Rosses Granitic complex, which also forms part of the Donegal Batholith, is shown in Figure 6f. K_1 orientations are horizontal to sub-horizontal and define a tight E-W orientated cluster (Figure 6fi). K_3 orientations are N-S directed and are horizontal (Figure 6fii).

The Trawenagh Bay Granite (Donegal Batholith): The youngest pluton in the Donegal Batholith is the Trawenagh Bay Granite, data for which is shown in Figure 6g. K_1 orientations form an E-W directed tight cluster and are predominantly horizontal (Figure 6gi), comparable to the marginally younger Rosses Granite. K_3 orientations are uniformly distributed along a well-defined marking a steep plane dipping East (Figure 6gii). Shape factor analysis shows samples dominantly recorded prolate ellipsoids, with greatest data density and samples recording the highest anisotropy, in the prolate field (Figure 6giii).

The Ross of Mull Granite: Results for the Ross of Mull Granite, of comparable age to the Omey Pluton in Ireland, are shown in Figure 6h. K_1 orientations broadly form a N-S directed girdle with directions predominantly plunging south (Figure 6hi). K_3 orientations define a tight E-W trending, horizontal cluster (Figure 6hii). Shape factor analysis shows samples equally record oblate and prolate ellipsoids (Figure 6hiii).

The Criffel Pluton: Results for the Criffel pluton, the youngest pluton studied, are shown in Figure 6i. No ellipsoid shape parameters were available. K_1 orientations define a wide NE-SW trending girdle (Figure 6ii). K_3 orientations are largely scatter in azimuth but show a consistent shallow plunge (Figure 6iii).

The Ratagain Granite: Results for the Ratagain Granite are shown in Figure 6j. K_1 orientations form a poorly defined N-S trending girdle with plunges varying from horizontal to vertical (Figure 6ji). K_3 orientations form an elongate cluster of horizontal points with directions ranging from E-W to NW-SE (Figure 6jii). Shape factor analysis shows almost exclusive oblate ellipsoids (Figure 6jiii).

5 Discussion

5.1 Variscan French Massif Central (FMC)

5.1.1 Comparison with regional tectonics

Within the FMC, the onset of post orogenic collapse was coincident with the ascent and emplacement of granitoid bodies between 325 – 310 Ma. During this period the main body of the FMC experienced NW-SE directed orogen parallel extension, whilst within the Cévennes region extension was E-W directed (*Talbot et al.*, 2000). If magmatic fabrics recorded by AMS data from FMC plutons are recording the regional syn-magmatic tectonic stress field then all fabrics would be expected to record extension, with NW-SE and E-W directed magnetic lineation in the main FMC and the Cévennes region respectively.

Alongside the regional tectonic regime, local variations in this stress field may be tested by comparing AMS fabrics to local contemporaneous strain markers. One significant marker is fabrics formed by metamorphic minerals within the thermal aureole of the pluton, as these will have developed as the magma body cooled and therefore formed within in the same syn-magmatic tectonic regime. As such if pluton scale AMS fabrics reliably record the regional tectonic stress field, approximate continuity should be expected between the fabric within the pluton and the fabric within the thermal aureole. Overall, where reported, mineral trends in thermal aureoles follow the regional tectonic trend (*Faure et al.*, 2009), meaning that tectonic AMS fabrics would also be expected to align with these mineral lineations.

Comparison with the regional tectonic stress field is best done through comparison with stereonets in Figures 3 and 4. Regionally, the FMC stereonets show approximately vertical to sub-vertical K_3 orientations, and a horizontal K_1 which would indicate horizontal stretching, which is being consistently recorded by pluton scale AMS fabrics across the FMC. Horizontal stretching is in keeping with the regional extensional post-orogenic collapse which occurred across the FMC during this time, as illustrated in Figures 7 and 8, which show stereonets for K_1 and K_3 respectively alongside the proposed tectonic history. Whilst the data does fit with direct extensional collapse it is also possible there was an element of transtension, or local transpression during this regime indicated by prolate deformation in a few plutons (e.g. Margeride Granitic Complex). Overall the pluton scale AMS fabrics across the FMC fit with the expected extensional tectonic regime.

The direction of the magnetic lineation recorded by AMS data can also be compared with the regional stretching lineation. Figure 9 shows project stereonets with K_1 contoured compared with the stretching direction recorded in host rocks by *Faure et al.* (2009). The orientation of the magnetic lineation recorded by the AMS data matches the trend of the host rock lineation. In the main FMC area, both K_1 orientations and the host rock lineation are NW-SE directed, whilst within the Cévennes region both are E-W directed (Figure 9), reliably following the regional tectonic extension direction. The consistency of axis orientations through time and space is also suggestive of a regional tectonic control.

The exception to this is the Rocles Pluton (Figure 4a), where K_1 is instead NE-SW directed. This divergence from the regional trend occurs as the pluton was tilted to the south by the later emplacement of the adjacent Velay Migmatite Dome (*Mezeme et al.*, 2007). Therefore, the measured fabric orientation is not the same as the orientation of the primary fabric at the time of formation. *Mezeme et al.* (2007) state that restoration to remove the effect of this later tilting would result in an average magmatic lineation striking N75°E, consistent with the E-W regional trend in the Cévennes region. This restoration has not been done quantitatively for all data so cannot be plotted but this average assessment suggests the Rocles pluton also records the regional tectonic trend (*Mezeme et al.*, 2007). Therefore, pluton-scale AMS fabrics in all plutons studied within the FMC reliably record both the extensional nature of the syn-magmatic regional tectonic regime and the direction of maximum extension (Figures 7 and 8).

The 332 $\pm$ 6 Ma Millevaches Granite Complex is notable as it straddles the 5 Km wide Pradines Fault Zone (Figure 2) a N-S directed ductile right-lateral strike-slip fault (*Gébelin et al.*, 2006). The Pradines Fault Zone has a significant effect on the internal structure of the granite complex, where lineation within, and directly adjacent to, the fault zone trending parallel to the fault strike (which is N-S) (*Gébelin et al.*, 2006). Outside the immediate fault zone, fabrics dominantly trend NW-SE (*Gébelin et al.*, 2006). This creates an overall sigmoidal shaped fabric with the magmatic lineation trending N-S in the centre of the pluton and NW-SE either side. The sigmoidal nature of this fabric led *Gébelin et al.* (2006) to conclude that fabric development in the Millevaches Complex was more influenced by the local dextral strike-slip faulting than the regional extension direction. However, as shown on Figures 7 and 8, at a pluton-scale the Millevaches Complex AMS data agrees with the regional tectonic extension direction and does not show significant differences from the other central FMC plutons analysed. Whilst a N-S trend in some data can be identified on Figure 3a, contouring shows that overall, this N-S fabric does not dominate the fabric, or appear to modify the mean orientation from the regional tectonic trend. It could be argued therefore, that instead of forming a sigmoidal pattern due to dextral shearing along the fault, the region outside the direct impact of the fault zone is recording the regional ambient tectonic strain field. Within the fault zone this is locally overprinted by deformation due to fault motions. Overall, the Millevaches Complex suggests that even in plutons significantly affected by local faulting, the regional tectonic stress field can be recorded by AMS fabrics. However, this may only occur due to the large size of the complex meaning the fault zone only affects a relatively small proportion.

The Glénat Pluton is a notable exception, with K_1 orientations being low angle (Figure 3c) indicative of regional extension but no clear clustering or orientation identifiable. Considering AMS data on a pluton scale leads to a significant spread in data due to local variations in the fabric within the pluton, such as local effects due to magma flow and pluton contacts. Therefore, even clustered data would be expected to show more spread than when considering single sites. Alongside this, *Joly et al.* (2009) report some solid-state deformation in the south of the pluton, due to the action of the Sillon

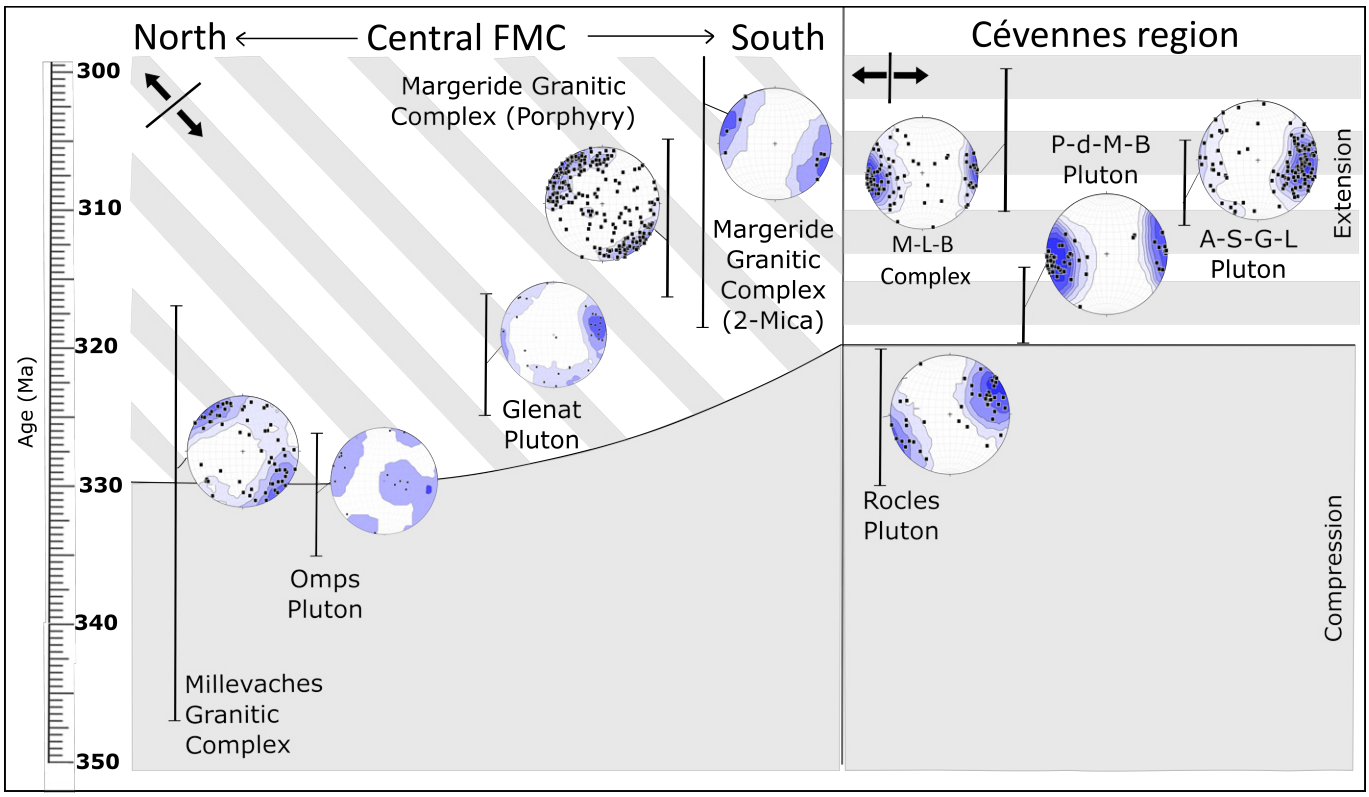

Figure 7 – Comparison between pluton-scale AMS fabrics as shown on stereonets from the nine plutons studied, with the K_1 (AMS lineation) orientation contoured and compared with the contemporaneous tectonic history for the French Massif Central. Age ranges for plutons (see Table1) are shown by black lines. Plutons from the main FMC and the Cévennes regions are distinguished, with plutons arranged from North to South from left to right. Extension direction is indicated by the black arrows (see Section 3.2).

Houiller Fault (Figure 2), which moved the Glénat 80 Km to the south following emplacement to its current location alongside the Omps pluton. This will have modified the primary emplacement fabric in the south of the pluton, which may explain the spread of K_1 orientations, although similar levels of post-emplacement deformation are reported for the Omps Pluton (Figure 3b) which more reliably records the regional stretching lineation. The low number of samples for this pluton may also have an impact on this interpretation.

5.1.2 Woodcock Analysis

Results of Woodcock analysis for all FMC plutons studied are shown in Figure 10. Overall, regionally K_1 values dominantly plot within the cluster field with only the Glénat Pluton, identified above as anomalous, plotting outside the cluster. Four out of seven K_3 values plot in the girdle field with no K_3 data available for the Glénat and Omps plutons. Overall, clustered K_1 orientations indicate a consistent σ_3 direction. This indicates a consistent extension direction being recorded across the plutons across the region, further suggesting fabrics are recording regional tectonic extension. C values indicate the degree of organisation within a sample, with larger values showing more organised samples. For both K_1 and K_3 almost all samples plot between the C=1 and C=2 lines, indicating some degree of organisation at a pluton scale. The Saint-Christophe-d'Allier Two-mica Granite is an outlier with a C value of 3.4 for K_3, indicating a stronger girdle distribution. Woodcock analysis agrees with analysis of stereonets indicating FMC plutons are recording regional tectonic extension.

The statistical significance of the fabric can also be analysed through comparison to critical values of *Woodcock and Naylor* (1983), as shown in Figure 11. Of the nine plutons all but the Omps Pluton record a significant fabric in both K_1 and K_3 at a 95% confidence limit and, of those, all but the Saint-Christophe-d'Allier Two-Mica Granite show a significant fabric at a 99% confidence limit (Figure 11). These two plutons both have less than 20 data points (N = 10 and N = 17 respectively) which likely accounts for the low statistical significance. This indicates significant fabric development at a pluton scale across FMC granites.

5.1.3 Ellipsoid Shape Factor

Plots of P_j vs T in Figure 3 shows that in the main FMC samples dominantly record oblate ellipsoids. Figure 4 shows that for the Cévennes region oblate ellipsoids also dominate but with a greater concentration of samples around T = 0, indicating a triaxial component to the strain field in this region. The slight modification of the regional strain field suggested by this may have

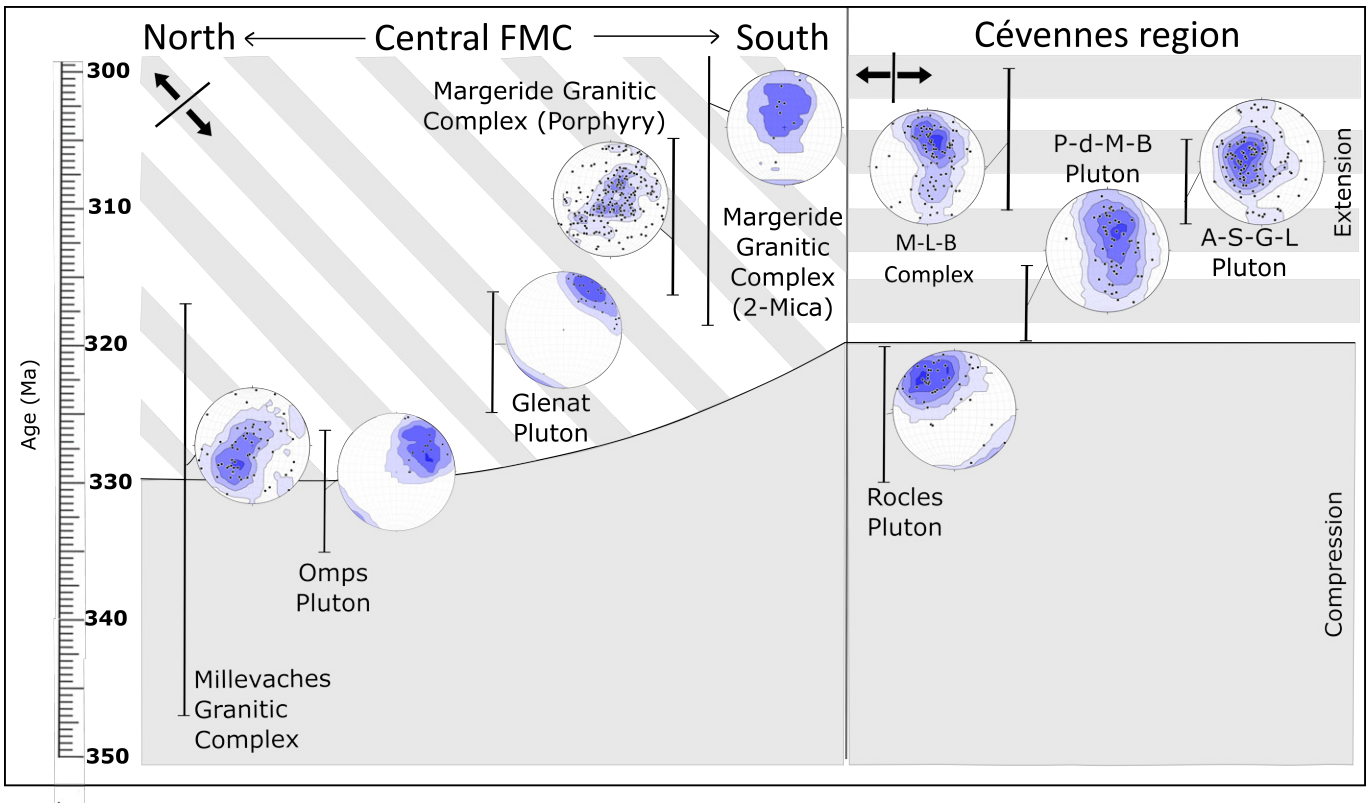

Figure 8 – Comparison between pluton-scale AMS fabrics as shown on stereonets from the nine plutons studied, with K_3 orientations (pole to AMS foliation) contoured and compared with the contemporaneous tectonic history for the French Massif Central. Age ranges for plutons (see Table1) are shown by black lines. K_3 orientation data for the Glénat and Omps Plutons is inferred from K_1 and K_2 values (see Appendix B). Plutons from the main FMC and the Cévennes regions are distinguished, with plutons arranged from North to South from left to right. Extension direction is indicated by the black arrows (see Section 3.2).

occurred to accommodate the differential stretching direction in this region from the rest of the FMC. In the main FMC, differential extension during the initial southwards propagation of extension was accommodated by sinistral strike-slip along the Sillon Houiller Fault (*Faure et al.*, 2009) but as no such structure separates the Cévennes region from the main FMC, the differences in extension will have affected the regional stress field more significantly, perhaps introducing an element of transtension into the extensional collapse.

Data points on these plots have also been coloured by susceptibility (K_m) value, where this data was available. The relationship between K_m and P_j can be used to indicate if changes in the degree of anisotropy are due to mineralogical changes (i.e. coupled changes in P_j and K_m) or due to changes in the stress field (changes in P_j do not correlate with changes in K_m). For the majority of the FMC granites there is no clear coupling between P_j and K_m. The Mont Lozére-Borne Granitic Complex and Glénat pluton potentially show a weak positive trend between P_j and K_m, potentially indicating a small mineralogical control on the anisotropy here but overall, the Figures 3 and 4 indicate the anisotropy recorded at the pluton scale is dominated by changes to the stress field.

There is however a contrast between the dominantly oblate ellipsoids recorded at an individual sample scale by P_j vs T plots and the pluton-scale fabric as analysed by Woodcock analysis (Figure 10). Woodcock analysis indicates regionally a cluster of K_1 orientations and a girdle of K_3 orientations, characteristic of prolate ellipsoids (*Tarling and Hrouda*, 1993) and as expected in extensional tectonic settings. Whilst oblate ellipsoids can form in response to tectonic extension recording vertical compression (i.e. crustal thinning) or compression along pluton margins in response to forceful emplacement, the differences indicated between individual samples sites and pluton scale fabrics are notable. Whilst the P_j vs T plot shows important information about the composition of the magnetic fabric at individual sites, as well as the ellipsoid shapes for these sites, it seems to less well capture the overall pluton-scale fabric. Hence, a true comparison of this pluton scale fabric to the regional tectonic field is better achieved by combining analysis methods, using P_j vs T plots, qualitatively comparisons with stereonets and the more quantitatively Woodcock analysis.

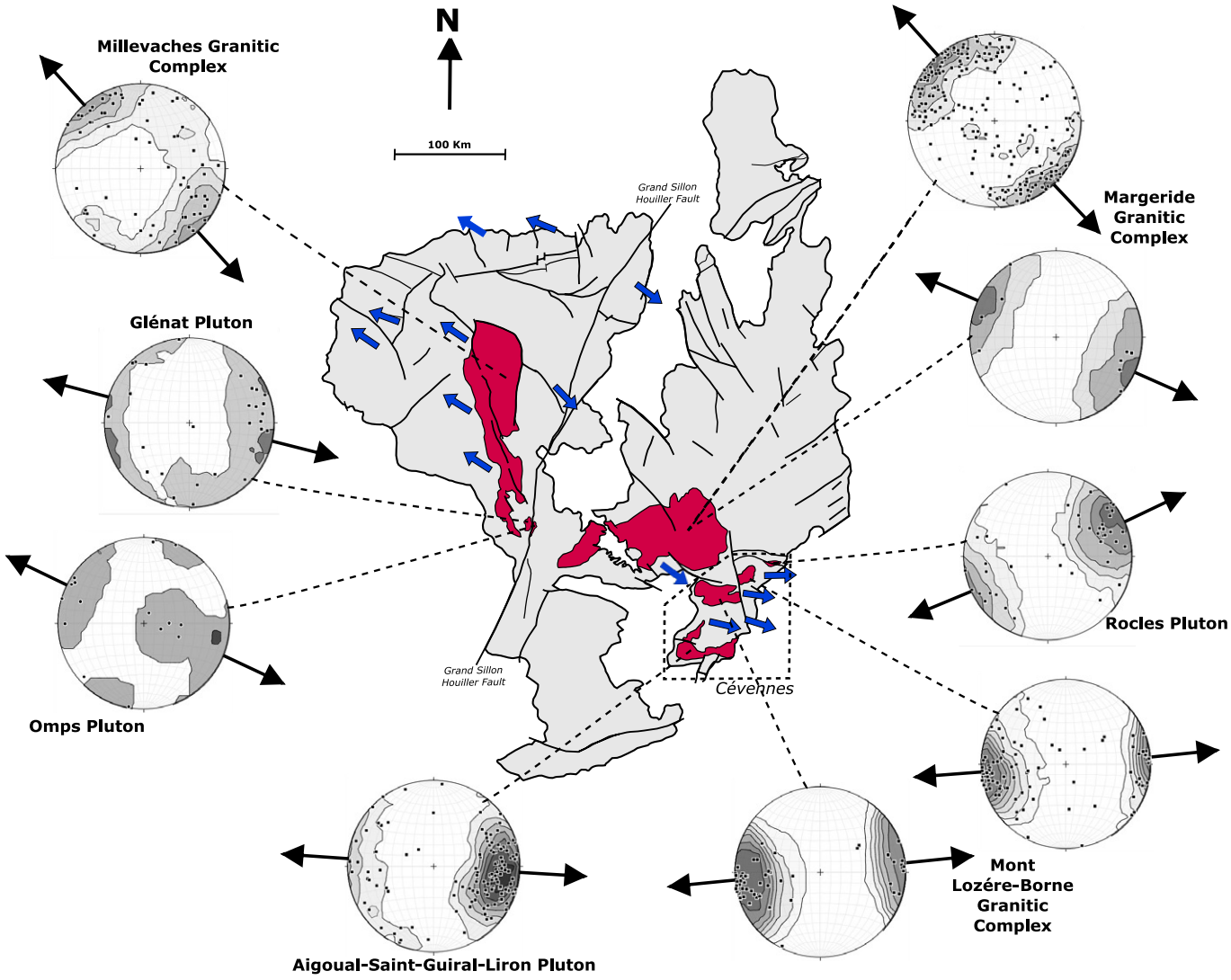

Figure 9 – Comparison between the orientation of the lineation recorded by pluton-scale AMS fabrics, shown on stereonets with K_1 contoured, with the trend of the lineation recorded in host rocks by *Faure et al.* (2009), shown by blue arrows. The Cévennes region is highlighted by the dashed box, and shows a different lineation trend from the rest of the FMC. The Rocles pluton does not match the regional trend as has been titled by the Velay migmatite dome (*Mezeme et al.*, 2007).

5.2 Caledonian Newer Granites of Scotland and Ireland

5.2.1 Comparison with Regional Tectonics

The Newer Granites of Scotland and Ireland were emplaced between 435 and 380 Ma (*Brown et al.*, 2008), during the final stages of the Caledonian orogeny, spanning a period of alternating tectonic regimes associated with the final oblique closure of the Iapetus Ocean and the onset of the Acadian orogeny. If AMS fabrics record the regional syn-magmatic tectonic regime, then any corresponding tectonic changes should be detectable in pluton-scale AMS data. This was tested through comparing the stereonets in Figure 6 with the concurrent regional tectonic regime. Figures 12 and 13 show a comparison between the tectonic frameworks of several authors) and K_1 and K_3 respectively.

The Ross of Mull Granite and the Omey pluton are of comparable age, emplaced during N-S directed sinistral Scandian Transpression, likely facilitated by transtensional jogs within this fault system during the final stages of Iapetus subduction (e.g., *Soper and Woodcock*, 2003; *Miles et al.*, 2016). At the pluton scale AMS fabric are comparable between the two plutons with K_3 orientations horizontal to sub-horizontal (Figure 13), as may form during homogenous orthogonal compression, and K_1 orientations forming a broadly N-S oriented girdle. There is more variation in K_1 with the Omey Pluton recording a NNW-SSE lineation and the Ross of Mull a NNE-SSW lineation. The Omey Pluton parallels the concurrent NNW-SSE shear zone which facilitated its emplacement (*McCarthy et al.*, 2015), as part of the regional sinistral transpression, showing the effect of local features within the regional field.

Another pluton of a comparable age is the Ardara pluton, which new U-Pb dating from *Archibald et al.* (2021) places at 431 to 424 Ma, a significant change from the previous date of 403 ± 8 Ma (*Siegesmund and Becker*, 2000). This new age also places the

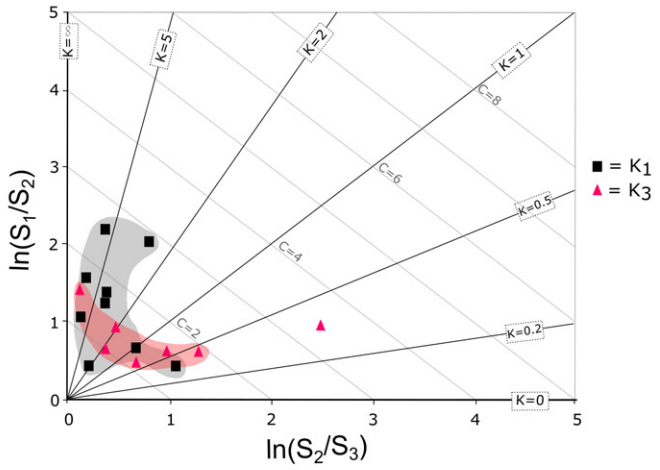

Figure 10 – Eigenvalue ratio plot from Woodcock analysis of FMC plutons, following procedure of *Woodcock and Naylor* (1983). Values for K_1 orientations are marked by a black square, and K_3 orientations with a pink triangle. The distribution of points is highlighted by the grey and pink shaded regions for K_1 and K_3 respectively, excluding one anomalously high value for K_3 from the Saint-Christophe-d'Allier two-mica granite.

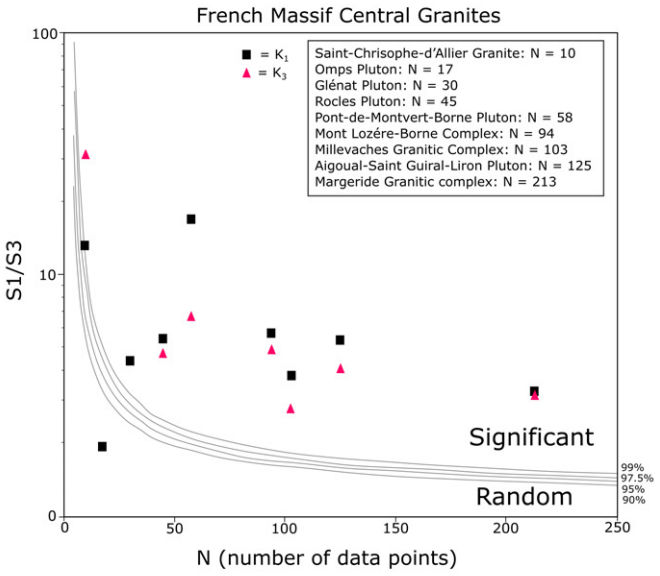

Figure 11 – Plot of S_1/S_3 values (plotted points) for the FMC plutons included in the project database compared to critical values of *Woodcock and Naylor* (1983) (curved lines), at 90%, 95%, 97.5% and 99% significance respectively. K_1 (square) and K_3 (triangle) are plotted for each pluton, with values plotting about the lines defined as statistically significant. All values apart from K_1 for the Omps pluton are statistically significant to 90% confidence limit, and all other values apart from K_1 for the Saint-Christophe-d'Allier Granite are significant at the 99% confidence limit showing over the AMS fabrics are statistically significant at a pluton scale.

Ardara pluton within Scandian transpression, using the framework of *Brown et al.* (2008).

However, Figure 12 shows the AMS fabric for Ardara is not comparable with the Ross of Mull or Omey, instead recording a distinct cluster of K_1 values. This would suggest triaxial strain with the overall ambient stretching component being oriented E-W and the compression component N-S, more comparable with later granites such as the Rosses Granite Complex. Overall, AMS data therefore seems to suggest that the Ardara pluton was instead emplaced during the period of sinistral transpression which followed the oblique convergence of the Iapetus Ocean. This suggests that convergence may have occurred earlier than 420 Ma (*Soper and Woodcock*, 2003; *Brown et al.*, 2008), in agreement with other authors (e.g., *Dewey and Strachan*, 2003; *Miles et al.*, 2016) who instead argued that it instead occurred at 425 Ma. Our datasets fit best when convergence occurs at this earlier time in the far SW, and then occurred progressively later to the NE, parallel to the Iapetus suture.

During the following period of transtension the Newry Igneous Complex and Donegal Batholith were emplaced. The Newry, Cloghoge, Ardara, Rosses and Trawenagh Bay plutons all record E-W clusters of K_1 orientations (Figure 12) and broadly N-S girdles of K_3 orientations (Figure 13), though these are more variably developed. Another pluton emplaced during this period of transtension is the Rathfriland Pluton. However AMS data for this pluton shows significant spread, and the absence of a well-defined K_1 fabric mean no tectonic interpretation can be made. Overall, the consistency between AMS fabrics in concurrent plutons located significant distances apart indicates the fabrics are reflecting regional stress fields. Alongside this, K_1 orientations are horizontal to sub-horizontal, indicating a horizontal minimum compressive stress as expected in extensional regimes. This is a clear switch from the earlier plutons, indicating the switch transpression to transtension immediately following Iapetus closure is recorded by pluton-scale AMS fabrics in the Irish granites.

The age range for the Trawenagh Bay Granite spans from this period of transtension to the onset of the Acadian Orogeny at around 400 Ma (*Dewey and Strachan*, 2003; *Brown et al.*, 2008; *Miles and Woodcock*, 2018), which lead to a short-lived period of transpression. The AMS fabric for Trawenagh Bay clearly matches the other plutons emplaced in the proceeding transtension, with a clear low angle cluster of K_1 orientations and an extremely well-developed girdle of K_3 orientations, so we place it in this regime at the older end of its potential age range.

During Acadian transpression the Criffel pluton was emplaced, and its AMS fabric shows a NE-SW girdle of K_1 orientations and broadly shallow plunging K_3 orientations, consistent with horizontal compression.

A similar fabric is seen in the data from the Ratagain Granite, with a broad N-S spread of K_1 orientations and NW-SE low-angle weakly clustered K_3 orientations. This fabric, also comparable with the Ross of Mull and Omey plutons, therefore, suggests

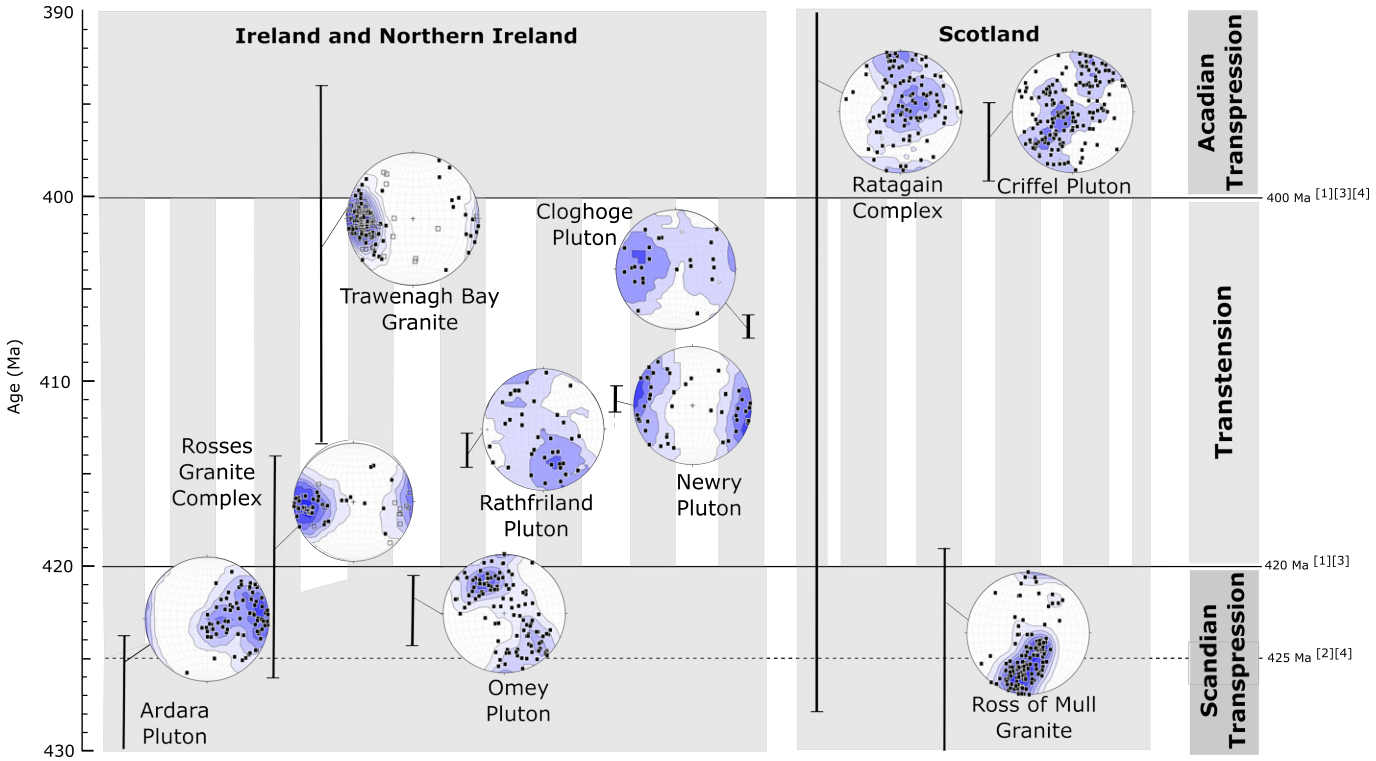

Figure 12 – Comparison between pluton-scale AMS fabrics as shown on stereonets, with K_1 orientation contoured, and the contemporaneous tectonic history, as reported by [1] *Soper and Woodcock* (2003), [2] *Dewey and Strachan* (2003), [3] *Brown et al.* (2008) and [4] *Miles et al.* (2016), respectively. The dotted line represents a potential earlier end to Scandian Transpression proposed by some authors at 425 Ma. Age ranges of the plutons (see Table 1) are represented by black lines, periods of transpression are highlighted by striped shading and transpression by solid colour. Plutons are ordered across the page from SW on the left to NE on the right, parallel to the Iapetus Suture (see Figure 5).

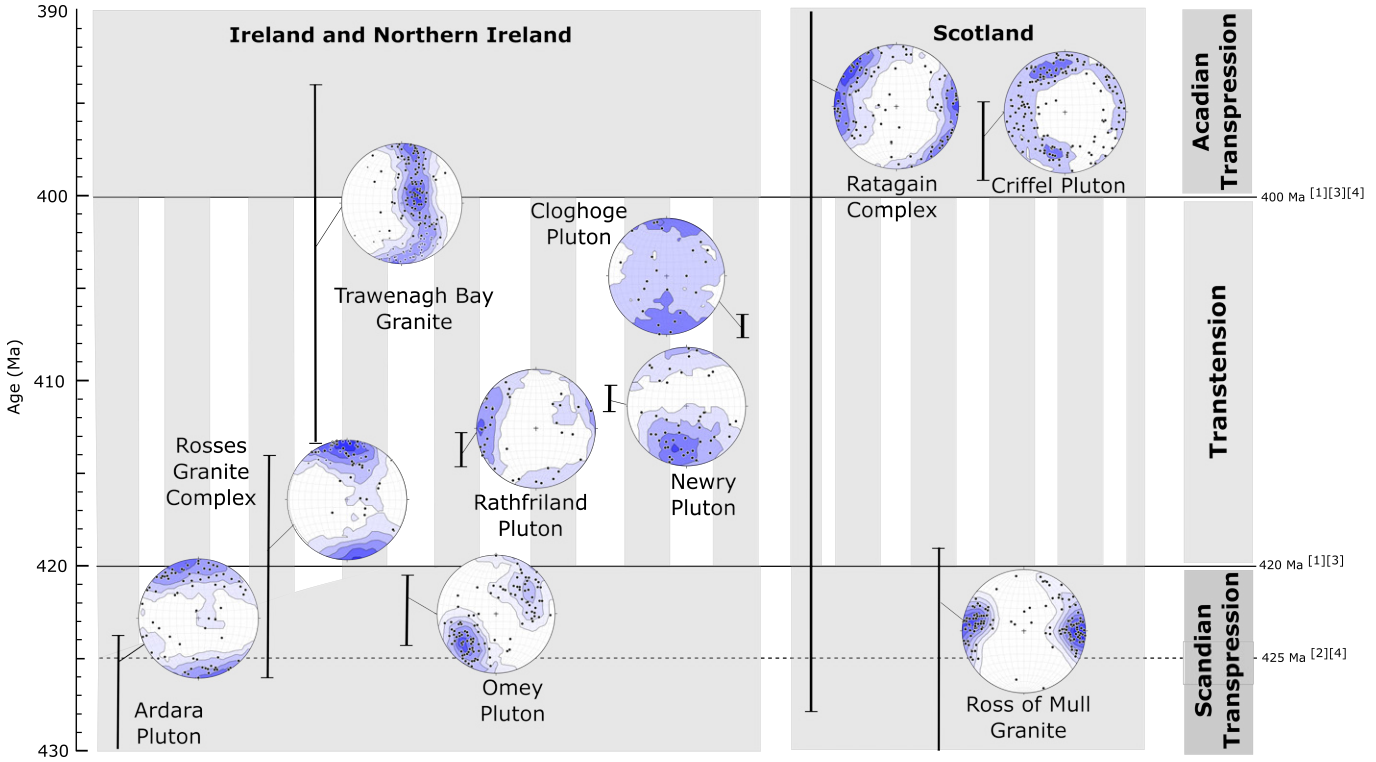

Figure 13 – Comparison between pluton-scale AMS fabrics as shown on stereonets, with K_3 orientation contoured, and the contemporaneous tectonic history, as reported by [1] *Soper and Woodcock* (2003), [2] *Dewey and Strachan* (2003), [3] *Brown et al.* (2008) and [4] *Miles et al.* (2016), respectively. The dotted line represents a potential earlier end to Scandian Transpression proposed by some authors at 425 Ma. Age ranges of the plutons (see Table 1) are represented by black lines periods of transpression are highlighted by striped shading and transpression by solid colour. Plutons are ordered across the page from SW on the left to NE on the right, parallel to the Iapetus Suture (see Figure 5).

that the Ratagain complex was also emplaced during a period of transpression, and agrees with the work of *Lawrence et al.* (2022) who reported the Ratagain as preserving a tectonic fabric formed during sinistral transpression. However, there is a significant spread of ages reported for the Ratagain Granite. The most recent U-Pb dates place the Ratagain emplacement as 425 ± 3 Ma (*Rogers and Dunning*, 1991), whereas *Pidgeon and Aftalion* (1978) instead place the complex much younger at 365 Ma. Taken in context with the regional tectonic framework and the transpressive AMS fabric, these ages therefore suggest that our data is compatible with Ratagain either being emplaced during the older Scandian transpression or the younger Acadian transpression (Figure 12). Assignment of Ratagain to either of these periods has no significant effect on our conclusions; both the geochronology and AMS fabric are compatible with the regional tectonic framework, as both indicate emplacement during a period of transpression, suggesting that the Ratagain granite too is recording the ambient tectonic strain field at a pluton scale. However, for completeness we must assign Ratagain to one tectonic period. Recent work (*Lawrence et al.*, 2022) indicates Ratagain was emplaced during Acadian transpression, on the basis of its geochemistry. *Lawrence et al.* (2022) analysed >100 samples from the complex, overall finding an enrichment in large-ion lithophile elements (LILE's) (e.g. Rb, Ba, K and Sr) and a depletion in high-field strength elements (e.g. U, Th, Nb, Zr, P, Ti) resulting in high Sr/Y and La/Yb ratios. This geochemical signature is characteristic of melts generated during slab-break off. Furthermore, *Lawrence et al.* (2022) also plotted tectonomagmatic discrimination diagrams (Rb vs. Nb + Y, Rb vs. Ta + Yb, Nb/Sr vs. Sr/Y and La/Yb vs. Sr/Y) (see Figures 11 to 12 in *Lawrence et al.*, 2022) all of which showed Ratagain plotted within the slab failure field. Slab failure has frequently been suggested as a method of melt generation for the late Caledonian granites (e.g., *Atherton*, 2002; *Miles et al.*, 2016; *Archibald et al.*, 2022), occurring following final convergence. On this basis we therefore assign the Ratagain granite to the younger Arcadian transpression, allowing us to fit both the transpressive tectonic regime recorded by the AMS fabric and the geochemical slab break off signal within the accepted regional tectonic framework.

However, there remains a need for an explanation for the ranges of dates calculated for the complex. Based on the above evidence Lawerence et al (2023) argue that the older date from *Rogers and Dunning* (1991) likely represents an early formed zircon within the crustal mush system present before final emplacement. Overall, we agree the Ratagain complex was emplaced during a period of transpression and tentatively place the complex within the younger Acadian transpression on the basis of this geochemical evidence but highlight the need for further geochronological work on this complex to fully resolve this uncertainty.

Overall, Figures 12 and 13 show that the pluton-scale AMS fabrics of the Caledonian Newer Granites of Scotland and Ireland clearly record the tectonic changes associated with final closure of the Iapetus Ocean. This indicates the effective use of pluton-scale AMS studies to clarify the timings of tectonic changes in regions with complex alternating tectonic regimes.

5.2.2 Woodcock Analysis

Results of Woodcock analysis for all Caledonian plutons are shown in Figure 14. The analysis shows little difference between overall K_1 and K_3 distributions, with C values typically between the C =1 and C=2 lines. K_1 and K_3 values for the Trawenagh Bay Granite are outliers, showing significantly more organisation than other plutons, as can be seen visually in Figure 6g.

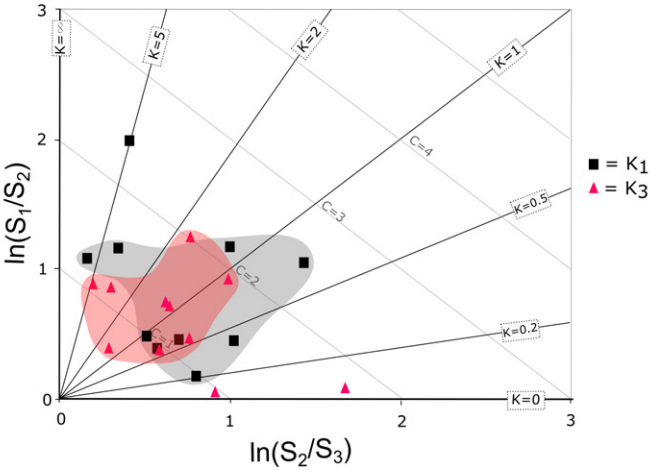

Figure 14 – Eigenvalue ratio plot from Woodcock Analysis of 'Newer Granite' plutons, following procedure of *Woodcock and Naylor* (1983). Values for K_1 orientations are marked by a black square, and K_3 orientations with a pink triangle. The distribution of points is highlighted by the grey and pink shaded regions for K_1 and K_3 respectively, excluding anomalously high values from the Trawenagh Bay Granite. No significant difference is seen between K_1 and K_3 where all plutons are considered together, regardless of the tectonic regime.

Comparison to the critical values of *Woodcock and Naylor* (1983) is shown in Figure 15. Of the ten granites studied, all but the Cloghoe and Rathfriland pluton (of the Newary Igneous Complex) record a statistically significant fabric distribution at a 99% confidence limit for both K_1 and K_3. As with the FMC granites, these represent the plutons with the lowest number of samples (N = 23 and N = 35 respectively). This again indicates that statistically significant fabrics are effectively resolved by AMS analysis at a pluton scale.

To determine if Woodcock analysis can quantify the effects of tectonic changes on pluton scale AMS fabrics, plutons were then grouped by tectonic regime during formation (as in Figures 12 and 13).

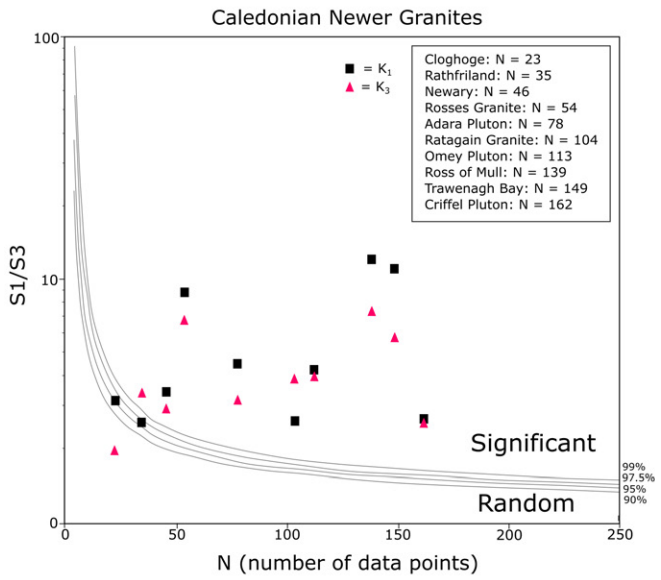

Figure 15 – Plot of S_1/S_3 values (plotted points) for the 'Newer Granite' plutons included in the project database compared to critical values of *Woodcock and Naylor* (1983) (curved lines) at 90%, 95%, 97.5% and 99% significance respectively. K_1 (square) and K_3 (triangle) are plotted for each pluton, with values plotting about the lines defined as statistically significant. All values apart from K_3 for the Cloghoge pluton are statistically significant to 90% confidence limit. Aside from K_1 for the Cloghoge and Rathfriland plutons all other values are statistically significant at the 99% confidence limit, showing AMS fabrics are statistically significant at a pluton scale.

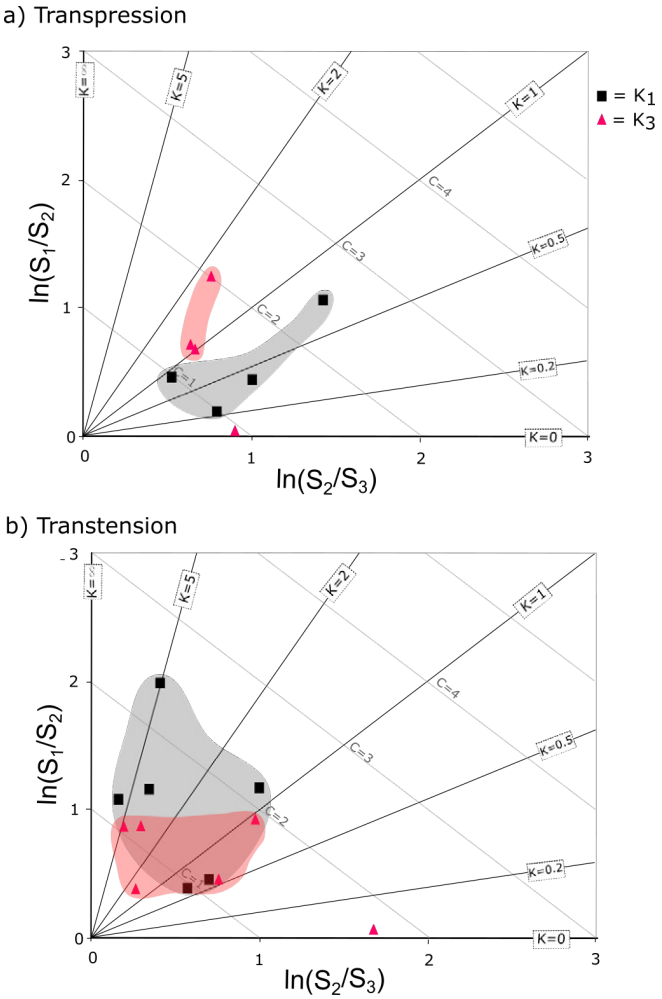

Figure 16 – Eigenvalue ratio plots from Woodcock Analysis of 'Newer Granite' plutons, following procedure of *Woodcock and Naylor* (1983). Values for K_1 orientations are marked by a black square, and K_3 orientations with a pink triangle. The distributions of points is highlighted by the grey and pink shaded regions for K_1 and K_3 respectively. **a)** Data from the Omey Pluton, Ross of Mull Granite and Criffel Pluton, emplaced during syn-magmatic transpression. **b)** Data from the Newary Igneous Complex and Donegal Batholith emplaced during syn-magmatic transtension.

This is shown in Figure 16. Plutons emplaced in transpressive tectonic regimes (Figure 15a) (Omey, Ross of Mull, Ratagain and Criffel) show K_1 values plotting exclusively in the girdle field. K_3 values plot dominantly in the cluster field, as expected in regions with a consistent maximum compression direction. The exception to this is the Criffel Pluton, highlighted above, again possibly indicating the weak nature of Acadian compression.

In contrast, plutons emplaced in transtensional tectonic regimes (Figure 15b) (Newry Igneous Complex and Donegal Batholith) overall show K_1 values in the cluster field which is expected in regions subjected to an extensional stress field. K_3 values plot more towards the girdle field, with 3 out of 6 plutons plotting here, though overall fabric organisations are more varied. Overall, Woodcock analysis shows a clear switch in fabric organisation corresponding to regional tectonic changes, demonstrating the utility of this analysis to quantitatively describe pluton scale fabric changes in response to changes to the regional tectonic strain field.

5.2.3 Ellipsoid Shape Factor

P_j-T plots in Figure 6 show a range of ellipsoid shapes recorded by individual samples, though most plutons are dominated by oblate ellipsoids. The changes correlating with regional tectonics seen on the stereonets (Figures 12 and 13) and Woodcock plots (Figure 15) are not seen in the ellipsoid shape parameters. This supports the earlier interpretation that ellipsoid shapes recorded by individual sites do not reflect the overall pluton-scale fabric, with local strain field variations dominating over regional tectonic stress at this scale. Colouring the data points by K_m values shows that for the majority of plutons there is no clear relationship between susceptibility and the degree of anisotropy, with changes in K_m values not correlating with changes in P_j. The exception is the Trawenagh Bay granite which does show a decrease in K_m value as P_j increases. Whilst this lack of clear relationship means a clear mineralogical control is not indicated by Figure 6 it is possible that it is possible that these tectonic changes could be better picked out on P_j vs T plots if mineralogical changes were more fully considered, as opposed to the simplified assumptions used in

this study to allow larger regional databased to be compiled.

5.3 Local Strain Heterogeneity

Localised strain heterogeneity will occur along internal contacts within plutons where mechanical contrasts occur (*Paterson et al.*, 1998), such as along the contact between different aged magma batches within a pluton (e.g., *Burton-Johnson et al.*, 2019). It is therefore relevant to consider the effect of such localised variations on the pluton scale AMS fabric compared to the overall regional tectonic strain field.

Burton-Johnson et al. (2019) found that for the Mt Kinabalu Pluton, tectonic fabrics dominated AMS data even at distances less than 5m from internal contacts, leading them to suggest that pluton-scale AMS fabrics could be related to syn-magmatic tectonic strain even if the internal pluton structure is unknown. We support this conclusion, with all AMS data points for a given pluton having been included in our analysis regardless of the location of the sample site in relation to either internal contacts or the pluton margin. The pervasive recording of the regional tectonic regime despite this indicates tectonic strain dominates over the impact of contact parallel fabrics and therefore detailed knowledge of the location of internal contacts is not required for reginal tectonic analysis.

This study also suggests a similar conclusion for other syn-magmatic structural features, such as fault zones and shear zones. The Millevaches Granite Complex records the regional tectonic regime at a pluton-scale despite the syn-magmatic action of the cross-cutting Pradines Fault Zone (Figure 2; *Gébelin et al.*, 2006). Immediately adjacent to the fault zone fabrics are fault parallel (*Gébelin et al.*, 2006) but at a pluton scale this local heterogeneity does not have an effect, with pluton scale AMS data for the Millevaches Granite Complex comparable to the other FMC plutons and the expected regional strain field, despite the heterogeneity in the fabric on the local scale. The same is seen in the Omey Pluton where AMS data reflects the expected regional tectonic strain field at a pluton-scale (Figure 6a) despite the action of two cross-cutting syn-magmatic shear zones (*McCarthy et al.*, 2015). In both cases all AMS datapoints from the original studies have been plotted on our stereonets, including those close to the shear zones, but the regional tectonic strain still dominates the overall signal. This illustrates that the overall tectonic fabric can be determined to a statistically significant level without the need to remove samples affected by localised simple shear, removing the need for potentially ambiguous choices about which data points to include. Similarly, this study shows that this is also the case in granites where prominent magma flow fabrics have been identified. One example of this is the Trawenagh Bay Granite, in which *Stevenson et al.* (2007) showed magnetic foliations recorded west directed magmatic flow lobes throughout the pluton. Even in such cases, where the tectonic fabric represents a smaller component of the stress field, this regional tectonic signal still forms a meaningful fabric, detectable at a pluton scale, without the need to isolate these samples.

6 Conclusions

Pluton-scale AMS fabrics in all nine plutons studied within the French Massif Central recorded the extensional phase of the Late Variscan orogenic collapse with magnetic lineations (K_1) parallel to the regional stretching direction. Pluton-scale AMS fabrics in nine plutons of the Caledonian 'Newer Granites' suite across Scotland and Ireland reliably record the tectonic changes between 430 and 390 Ma following the closure of the Iapetus Ocean, when compared to the accepted regional tectonic framework.

Changes in regional tectonics as recorded by pluton-scale AMS fabrics are statistically significant and can be detected at the pluton scale following the procedures of *Woodcock and Naylor* (1983). This allows statistical quantification of changes in AMS fabrics at a pluton scale. Even in plutons where the fabric is significantly affected by magma flow dynamics, such as the Trawenagh Bay Granite (*Stevenson et al.*, 2007), the regional tectonic regime can be determined from pluton-scale AMS fabrics.

This study found that the regional tectonic strain field was recorded pervasively by AMS fabrics in both study regions and that such comparison is best achieved qualitatively through comparisons between K_1 and K_3 on contoured equal area plots and more quantitatively through Woodcock analysis. Overall, this indicates there is significant potential to use pluton-scale AMS fabrics to study the evolution of regional tectonic strain fields. The Newer Granite's suite highlights the use of AMS fabrics and precise aging of granite plutons for recording and interpreting changes in regional tectonic regime. This suggests such a regional AMS analysis would have significant potential for use as a method to refine the timings of such events which previously have proved ambiguous.

Acknowledgements

This work formed part of H. Knight's thesis toward an MSci in Geology at the University of Birmingham. We would like to thank Helena Silva, Eric C. Ferré and Rob Strachan for their helpful comments which improved the quality of the manuscript. Editor Andy Parsons is also thanked for his assistance and useful comments.

Author contributions

All authors contributed to conceptualisation of ideas and methodology development, assisted with analysis of the AMS datasets, alongside contributing to writing and reviewing the manuscript. **Hazel Knight** compiled the database, carried out the initial analysis and wrote the first draft of the manuscript.

Data availability

All datasets exist as previously published work (see references in Table 1) and the compiled regional databases (Appendix A and B) are available at doi.org/10.6084/m9.figshare.23742207.v1.

Competing interests

The authors declare no competing interests.

Peer review

This publication was peer-reviewed by Eric C. Ferré, Helena Silva, and Rob Strachan. The full peer-review report can be found here: Review Report.

Copyright notice

References

Anderson, P. (2015), Zonation and emplacement of the Newry igneous complex, Nothern Ireland, Ph.D. thesis, University of Birmingham, United Kingdom.

Anderson, P. E., C. T. Stevenson, M. R. Cooper, I. G. Meighan, R. J. Reavy, C. T. Hurley, J. Inman, and R. M. Ellam (2018), Refined model of incremental emplacement based on structural evidence from the granodioritic Newry igneous complex, Northern Ireland, *GSA Bulletin*, *130*(5-6), 740–756, doi: 10.1130/B31756.1.

Archanjo, C. J., J.-L. Bouchez, M. Corsini, and A. Vauchez (1994), The Pombal granite pluton: Magnetic fabric, emplacement and relationships with the Brasiliano strike-slip setting of NE Brazil (Paraiba State), *Journal of structural geology*, *16*(3), 323–335, doi: 10.1016/0191-8141(94)90038-8.

Archibald, D. B., L. M. G. Macquarrie, J. B. Murphy, R. A. Strachan, C. R. M. McFarlane, M. Button, K. P. Larson, and J. Dunlop (2021), The construction of the Donegal composite batholith, Irish Caledonides: Temporal constraints from U-Pb dating of zircon and titanite, *Geological Society of America bulletin*, *133*(11-12), 2335–2354, doi: 10.1130/b35856.1.

Archibald, D. B., J. B. Murphy, M. Fowler, R. A. Strachan, and R. S. Hildebrand (2022), Testing petrogenetic models for contemporaneous mafic and felsic to intermediate magmatism within the "Newer Granite" suite of the Scottish and Irish Caledonides, in *New Developments in the Appalachian-Caledonian-Variscan Orogen*, edited by Y. D. Kuiper, J. B. Murphy, R. D. Nance, R. A. Strachan, and M. D. Thompson, pp. 375–399, Geological Society of America, doi: 10.1130/2021.2554(15).

Atherton, M. (2002), Slab breakoff: a model for Caledonian, Late Granite syn-collisional magmatism in the orthotectonic (metamorphic) zone of Scotland and Donegal, Ireland, *Lithos*, *62*(3-4), 65–85, doi: 10.1016/s0024-4937(02)00111-1.

Augay, J. F. (1979), Les leucogranites et monzogranites de la region d'Eymoutiers–Peyrat le Château (Massif du Millevaches, Massif Central Français), Ph.D. thesis, University of Lyon I, Lyon, France.

Beckinsale, R. D., and J. D. Obradovich (1973), Potassium-argon ages for minerals from the Ross of Mull, Argyllshire, Scotland, *Scottish journal of geology*, *9*(2), 147–156.

Benn, K., S. R. Paterson, S. P. Lund, G. S. Pignotta, and S. Kruse (2001), Magmatic fabrics in batholiths as markers of regional strains and plate kinematics: example of the Cretaceous Mt. Stuart batholith, *Physics and Chemistry of the Earth Part A Solid Earth and Geodesy*, *26*(4-5), 343–354, doi: 10.1016/s1464-1895(01)00064-3.

Biedermann, A., and D. Bilardello (2021), Practical Magnetism VII: Avoiding common misconceptions in magnetic fabric interpretation, *The IRM Quarterly*.

Borradaile, G. J., and B. Henry (1997), Tectonic applications of magnetic susceptibility and its anisotropy, *Earth-science reviews*, *42*(1-2), 49–93, doi: 10.1016/s0012-8252(96)00044-x.

Borradaile, G. J., and M. Jackson (2004), Anisotropy of magnetic susceptibility (AMS): magnetic petrofabrics of deformed rocks, *Geological Society special publication*, *238*(1), 299–360, doi: 10.1144/gsl.sp.2004.238.01.18.

Bouchez, J. L. (1997), *Granite is never isotropic: an introduction to AMS studies of granitic rocks. In Granite: from segregation of melt to emplacement fabrics*, Springer, Berlin, Germany.

Brown, P. E., P. D. Ryan, N. J. Soper, and N. H. Woodcock (2008), The Newer Granite problem revisited: a transtensional origin for the Early Devonian trans-suture suite, *Geological magazine*, *145*(2), 235–256, doi: 10.1017/S0016756807004219.

Burton-Johnson, A., C. G. Macpherson, J. R. Muraszko, R. J. Harrison, and T. A. Jordan (2019), Tectonic strain recorded by magnetic fabrics (AMS) in plutons, including Mt Kinabalu, Borneo: A tool to explore past tectonic regimes and syn-magmatic deformation, *Journal of structural geology*, *119*, 50–60, doi: 10.1016/j.jsg.2018.11.014.

Cashman, K. V., R. S. J. Sparks, and J. D. Blundy (2017), Vertically extensive and unstable magmatic systems: A unified view of igneous processes, *Science (New York, N.Y.)*, *355*(6331), eaag3055, doi: 10.1126/science.aag3055.

Couturié, J. P., M. Caen-Vachette, and Y. Vialette (1979), Age namurien d'un laccolite granitique différencié par gravité: le granite de la Margeride (M. C. F.), *Comptes Rendus de l'Académie des Sciences*, *289*, 449–452.

de Saint Blanquat, M., and B. Tikoff (1997), Development of magmatic to solid-state fabrics during syntectonic emplacement of the mono creek granite, Sierra

Nevada batholith, in *Petrology and Structural Geology*, vol. 8, edited by J. L. Bouchez, D. H. W. Hutton, and W. E. Stephens, pp. 231–252, Springer Netherlands, Dordrecht, doi: 10.1007/978-94-017-1717-5_15.

Dewey, J. F., and R. A. Strachan (2003), Changing Silurian–Devonian relative plate motion in the Caledonides: sinistral transpression to sinistral transtension, *Journal of the Geological Society*, *160*(2), 219–229, doi: 10.1144/0016-764902-085.

Dunlop, D., and O. Ozdemir (1997), *Rock magnetism*, pp 1–573, Cambridge University Press, Cambridge, England.

Faure, M. (1995), Late orogenic carboniferous extensions in the Variscan French Massif Central, *Tectonics*, *14*(1), 132–153, doi: 10.1029/94TC02021.

Faure, M., X. Charonnat, A. Chauvet, Y. Chen, J.-Y. Talbot, G. Martelet, G. Courrioux, P. Monie, and J.-P. Milesi (2001), Tectonic evolution of the Cevennes para-autochthonous domain of the Hercynian French Massif Central and its bearing on ore deposits formation, *Bulletin de la Societe Geologique de France*, *172*(6), 687–696, doi: 10.2113/172.6.687.

Faure, M., E. Bé Mézème, M. Duguet, C. Cartier, and J.-Y. Talbot (2005), Paleozoic tectonic evolution of medio-Europa from the example of the French Massif Central and Massif Armoricain, *Journal of the virtual explorer*, *19*(5), 1–25, doi: 10.3809/jvirtex.2005.00120.

Faure, M., J.-M. Lardeaux, and P. Ledru (2009), A review of the pre-Permian geology of the Variscan French Massif Central, *Comptes rendus: Geoscience*, *341*(2-3), 202–213, doi: 10.1016/j.crte.2008.12.001.

Feely, M., D. Selby, J. Conliffe, and M. Judge (2007), Re–Os geochronology and fluid inclusion microthermometry of molybdenite mineralisation in the late-Caledonian Omey Granite, western Ireland, *Transactions of the Institution of Mining and Metallurgy, Section B*, *116*(3), 143–149, doi: 10.1179/174327507x207465.

Gébelin, A., G. Martelet, Y. Chen, M. Brunel, and M. Faure (2006), Structure of late Variscan Millevaches leucogranite massif in the French Massif Central: AMS and gravity modelling results, *Journal of structural geology*, *28*(1), 148–169, doi: 10.1016/j.jsg.2005.05.021.

Halliday, A. N., W. E. Stephens, and R. S. Harmon (1980), Rb-Sr and O isotopic relationships in 3 zoned Caledonian granitic plutons, Southern Uplands, Scotland: evidence for varied sources and hybridization of magmas, *Journal of the Geological Society*, *137*(3), 329–348, doi: 10.1144/gsjgs.137.3.0329.

Isnard, H. (1996), Datation par la méthode U–Pb sur monazites des granites du Mont Lozére et de l'Est de la Margeride (laccolites de Chambon-le-Château et de St-Christophe d'Allier): contribution á l'histoire post tectonique du Massif Central Français, Master's thesis, Université de Montpellier II, Montpellier, France.

Jacques, J. M., and R. J. Reavy (1994), Caledonian plutonism and major lineaments in the SW Scottish Highlands, *Journal of the Geological Society*, *151*(6), 955–969, doi: 10.1144/gsjgs.151.6.0955.

Jelinek, V. (1981), Characterization of the magnetic fabric of rocks, *Tectonophysics*, *79*(3-4), T63–T67, doi: 10.1016/0040-1951(81)90110-4.

Jelínek, V. (1977), *The statistical theory of measuring anisotropy of magnetic susceptibility of rocks and its application*, *[Produits pharmaceutiques]*, vol. 29, Geofyzika, [object Object].

Jelínek, V. (1978), Statistical processing of anisotropy of magnetic susceptibility measured on groups of specimens, *Studia geophysica et geodaetica*, *22*(1), 50–62, doi: 10.1007/bf01613632.

Joly, A., M. Faure, G. Martelet, and Y. Chen (2009), Gravity inversion, AMS and geochronological investigations of syntectonic granitic plutons in the southern part of the Variscan French Massif Central, *Journal of structural geology*, *31*(4), 421–443, doi: 10.1016/j.jsg.2009.01.004.

Lawrence, A., M. Maffione, and C. T. E. Stevenson (2022), Mush ado about the Ratagain Complex, NW Scotland: insights into Caledonian granitic magmatism and emplacement from magnetic fabric analyses, *Scottish journal of geology*, *58*(1), sjg2021–018, doi: 10.1144/sjg2021-018.

Marre, J. (1986), Structural analysis of granitic rocks, *International journal of rock mechanics and mining sciences & geomechanics abstracts*, *23*(5), 171, doi: 10.1016/0148-9062(86)90022-7.

McAteer, C. A. (2009), Provenance of metasedimentary sequences in the Scottish and Irish Caledonides, Ph.D. thesis, University College Dublin.

McCarthy, W., R. J. Reavy, C. T. Stevenson, and M. S. Petronis (2015), Late Caledonian transpression and the structural controls on pluton construction; new insights from the Omey Pluton, western Ireland, *Earth and environmental science transactions of the Royal Society of Edinburgh*, *106*(1), 11–28, doi: 10.1017/s1755691015000201.

McCarthy, W. J. (2013), An evaluation of orogenic kinematic evolution utilizing crystalline and magnetic anisotropy in granitoids, Ph.D. thesis, National University of Ireland, Cork, Ireland.

Mezeme, E. B., M. Faure, A. Cocherie, and Y. Chen (2005), *In situ* chemical dating of tectonothermal events in the French Variscan Belt, *Terra nova*, *17*(5), 420–426, doi: 10.1111/j.1365-3121.2005.00628.x.

Mezeme, E. B., M. Faure, Y. Chen, A. Cocherie, and J.-Y. Talbot (2007), Structural, AMS and geochronological study of a laccolith emplaced during Late Variscan orogenic extension: the Rocles pluton (SE French Massif Central), *International journal of earth sciences*, *96*(2), 215–228, doi: 10.1007/s00531-006-0098-2.

Mialhe, J. (1980), Le massif granitique de la Borne: étude pétrographique, géochimique, géochronologique et structurale, Ph.D. thesis, Université de Clermont-Ferrand, France.

Miles, A. J., and N. H. Woodcock (2018), A combined geochronological approach to investigating long lived granite magmatism, the Shap granite, UK, *Lithos*, *304-307*, 245–257, doi: 10.1016/j.lithos.2018.02.012.

Miles, A. J., N. H. Woodcock, and C. J. Hawkesworth (2016), Tectonic controls on post-subduction granite genesis and emplacement: The late Caledonian suite of Britain and Ireland, *Gondwana research: international geoscience journal*, *39*, 250–260, doi: 10.1016/j.gr.2016.02.006.

Monier, G. (1980), Pétrologie des granitoïdes du Sud Millevaches (Massif Central Français). Minéralogie, géochimie, géochronologie, *Theśe*, *3éme Cycle, Uniersité de Clermont II*.

Monié, P., J. P. Respaut, S. Brichaud, V. Bouchot, M. Faure, and J. Y. Roig (2000), 40Ar/39Ar and U-Pb geochronology applied to Au-W-Sb metallogenesis in the Cévennes and Châtaigneraie districts (Southern Massif Central, France), *Documents du BRGM. Substance minérales et énergétiques*,

297(297), 77–79.

Neilson, J. C., B. P. Kokelaar, and Q. G. Crowley (2009), Timing, relations and cause of plutonic and volcanic activity of the Siluro-Devonian post-collision magmatic episode in the Grampian Terrane, Scotland, *Journal of the Geological Society*, *166*(3), 545–561, doi: 10.1144/0016-76492008-069.

O'Driscoll, B., C. T. E. Stevenson, and V. R. Troll (2008), Mineral lamination development in layered gabbros of the British Palaeogene igneous province: A combined anisotropy of magnetic susceptibility, quantitative textural and mineral chemistry study, *Journal of petrology*, *49*(6), 1187–1221, doi: 10.1093/petrology/egn022.

Oliver, G. J. H., S. A. Wilde, and Y. Wan (2008), Geochronology and geodynamics of Scottish granitoids from the late Neoproterozoic break-up of Rodinia to Palaeozoic collision, *Journal of the Geological Society*, *165*(3), 661–674, doi: 10.1144/0016-76492007-105.

Owens, W. H. (2000), Error estimates in the measurement of anisotropic magnetic susceptibility, *Geophysical journal international*, *142*(2), 516–526, doi: 10.1046/j.1365-246x.2000.00175.x.

Owens, W. H., and D. Bamford (1976), A Discussion on natural strain and geological structure - Magnetic, seismic, and other anisotropic properties of rock fabrics, *Philosophical transactions of the Royal Society of London*, *283*(1312), 55–68, doi: 10.1098/rsta.1976.0069.

Parsons, A., E. Ferré, R. Law, G. Lloyd, R. Phillips, and M. Searle (2016), Orogen-parallel deformation of the Himalayan midcrust: Insights from structural and magnetic fabric analyses of the Greater Himalayan Sequence, Annapurna-Dhaulagiri Himalaya, central Nepal, *Tectonics*, *35*(11), 2515–2537, doi: 10.1002/2016TC004244.

Paterson, S. R., T. K. Fowler, Jr, K. L. Schmidt, A. S. Yoshinobu, E. S. Yuan, and R. B. Miller (1998), Interpreting magmatic fabric patterns in plutons, *Lithos*, *44*(1-2), 53–82, doi: 10.1016/s0024-4937(98)00022-x.

Petford, N. (2003), Rheology of granitic magmas during ascent and emplacement, *Annual review of earth and planetary sciences*, *31*(1), 399–427, doi: 10.1146/annurev.earth.31.100901.141352.

Petford, N., A. R. Cruden, K. J. McCaffrey, and J. L. Vigneresse (2000), Granite magma formation, transport and emplacement in the Earth's crust, *Nature*, *408*(6813), 669–673, doi: 10.1038/35047000.

Petronis, M. S., B. O'Driscoll, C. T. E. Stevenson, and R. J. Reavy (2012), Controls on emplacement of the Caledonian Ross of Mull Granite, NW Scotland: Anisotropy of magnetic susceptibility and magmatic and regional structures, *GSA Bulletin*, *124*(5-6), 906–927, doi: 10.1130/B30362.1.

Pidgeon, R. T., and M. Aftalion (1978), Inherited zircon U-Pb system as indicators of granite souce rocks in the British Caledonides, in *IV Int Conf Geochron Cosmochron Isot Geol Aspen*, pp. 335–336.

Pin, C. (1979), Géochronologie U–Pb et microtectonique des series métamorphiques ante´ste´phaniennes de l'Aubrac et de la région de Marvejols (Massif Central), Ph.D. thesis, Université de Montpellier, Montpellier, France.

Pitcher, W. S. (1997), *The nature and origin of granite*, Springer My Copy UK.

Porter, E. M. (2002), Anisotrophy of Magnetic Susceptibility in the Criffel-Dalbeattie Pluton, Scotland: Implications for Emplacement Mechanism, Ph.D. thesis, University of Birmingham.

Respaut, J. P. (1984), Géochronologie et géochimie isotopique U–Pb de la minéralisation uranifére de la mine des Pierres Plantées (Lozére) et de son encaissant: le massif granitique de la Margeride, Ph.D. thesis, Université de Montpellier, Montpellier, France.

Rochette, P. (1987), Magnetic susceptibility of the rock matrix related to magnetic fabric studies, *Journal of structural geology*, *9*(8), 1015–1020, doi: 10.1016/0191-8141(87)90009-5.

Rogers, G., and G. R. Dunning (1991), Geochronology of appinitic and related granitic magmatism in the W Highlands of Scotland: constraints on the timing of transcurrent fault movement, *Journal of the Geological Society*, *148*(1), 17–27, doi: 10.1144/gsjgs.148.1.0017.

Schulmann, K., J.-B. Edel, J. R. Martínez Catalán, S. Mazur, A. Guy, J.-M. Lardeaux, P. Ayarza, and I. Palomeras (2022), Tectonic evolution and global crustal architecture of the European Variscan belt constrained by geophysical data, *Earth-science reviews*, *234*(104195), 104,195, doi: 10.1016/j.earscirev.2022.104195.

Searle, M. P. (2022), Tectonic evolution of the Caledonian orogeny in Scotland: a review based on the timing of magmatism, metamorphism and deformation, *Geological magazine*, *159*(1), 124–152, doi: 10.1017/s0016756821000947.

Siegesmund, S., and J. K. Becker (2000), Emplacement of the Ardara pluton (Ireland): new constraints from magnetic fabrics, rock fabrics and age dating, *International journal of earth sciences*, *89*(2), 307–327, doi: 10.1007/s005310000088.

Soper, N. J., and N. H. Woodcock (2003), The lost Lower Old Red Sandstone of England and Wales: a record of post-Iapetan flexure or Early Devonian transtension?, *Geological magazine*, *140*(6), 627–647, doi: 10.1017/S0016756803008380.

Sparks, R. S. J., C. Annen, J. D. Blundy, K. V. Cashman, A. C. Rust, and M. D. Jackson (2019), Formation and dynamics of magma reservoirs, *Philosophical transactions. Series A, Mathematical, physical, and engineering sciences*, *377*(2139), 20180,019, doi: 10.1098/rsta.2018.0019.

Stevenson, C. (2009), The relationship between forceful and passive emplacement: The interplay between tectonic strain and magma supply in the Rosses Granitic Complex, NW Ireland, *Journal of structural geology*, *31*(3), 270–287, doi: 10.1016/j.jsg.2008.11.009.

Stevenson, C. T., W. H. Owens, and D. H. Hutton (2007), Flow lobes in granite: The determination of magma flow direction in the Trawenagh Bay Granite, northwestern Ireland, using anisotropy of magnetic susceptibility, *Geological Society of America bulletin*, *119*(11-12), 1368–1386, doi: 10.1130/B25970.1.

Talbot, J.-Y., Y. Chen, M. Faure, and W. Lin (2000), AMS study of the Pont-de-Montvert-Borne porphyritic granite pluton (French Massif Central) and its tectonic implications, *Geophysical journal international*, *140*(3), 677–686, doi: 10.1046/j.1365-246x.2000.00067.x.

Talbot, J.-Y., G. Martelet, G. Courrioux, Y. Chen, and M. Faure (2004), Emplacement in an extensional setting of the Mont Lozère–Borne granitic complex (SE France) inferred from comprehensive AMS, structural and gravity studies, *Journal of structural geology*, *26*(1), 11–28, doi:

10.1016/s0191-8141(03)00083-x.

Talbot, J.-Y., M. Faure, Y. Chen, and G. Martelet (2005a), Pull-apart emplacement of the Margeride granitic complex (French Massif Central). Implications for the late evolution of the Variscan orogen, *Journal of structural geology*, *27*(9), 1610–1629, doi: 10.1016/j.jsg.2005.05.008.

Talbot, J. Y., Y. Chen, and M. Faure (2005b), A magnetic fabric study of the Aigoual–Saint Guiral–Liron granite pluton (French Massif Central) and relationships with its associated dikes, *Journal of Geophysical Research: Solid Earth*, *110(B12)*, doi: 10.1029/2005JB003699.

Tarling, D. H., and F. Hrouda (1993), *Magnetic Anisotropy of Rocks*, 1993 ed., Chapman and Hall, London, England.

Thirlwall, M. F. (1988), Geochronology of Late Caledonian magmatism in northern Britain, *Journal of the Geological Society*, *145*(6), 951–967, doi: 10.1144/gsjgs.145.6.0951.

Turnell, H. B. (1985), Palaeomagnetism and Rb–Sr ages of the Ratagan and Comrie intrusions, *Geophysical journal international*, *83*, 363–378, doi: 10.1111/j.1365-246X.1985.tb06492.x.

Vigneresse, J., and J. D. Clemens (2000), Granitic magma ascent and emplacement: neither diapirism nor neutral buoyancy, *Geological Society special publication*, *174*(1), 1–19, doi: 10.1144/GSL.SP.1999.174.01.01.

Vigneresse, J. L., P. Barbey, and M. Cuney (1996), Rheological transitions during partial melting and crystallization with application to felsic magma segregation and transfer, *Journal of petrology*, *37*(6), 1579–1600, doi: 10.1093/petrology/37.6.1579.

Woodcock, N. H., and M. A. Naylor (1983), Randomness testing in three-dimensional orientation data, *Journal of structural geology*, *5*(5), 539–548, doi: 10.1016/0191-8141(83)90058-5.

Woodcock, N. H., and R. A. Strachan (2012), *Geological history of Britain and Ireland*, second ed., John Wiley Sons.